Phenotypic and genotypic study of hypervirulent *Klebsiella pneumoniae* (hvKp) and molecular characterization of its resistance and virulence determinants.

Master's Thesis
Daniela Vallejo Iriarte

Supervisor**: Alain Antonio Ocampo Sosa**
Co-Supervisor**: Sergio García Fernández**

Date: 7 of June, 2024

Interuniversity Master's Degree in Biomedicine and Molecular Biology

Servicio de Microbiología. Hospital Universitario Marqués de Valdecilla-IDIVAL

INDEX

ABSTRACT

Hypervirulent *Klebsiella pneumoniae* (hvKp) has emerged as a significant pathogen due to its increasing incidence. Originally considered an opportunistic bacterium responsible for nosocomial infections in immunocompromised individuals, it now poses a substantial threat by causing severe infections, such as pneumonia, liver abscesses, or bacteremia, in previously healthy individuals. To comprehend the genetic and phenotypic basis of this virulence, we performed both phenotypic and genotypic characterization in hvKp identified during daily routine screening of suspected hvKp isolates in a university hospital in Spain to i) identify genes related to resistance and virulence, ii) quantify biofilm formation, iii) measure motility, iv) conduct conjugation assays, and v) assess the virulence potential in infected *Galleria mellonella* larvae. Whole-genome sequencing results revealed a high prevalence of key genes in both virulence (*magA*, *wzy_K2*, *fim*) and resistance (*fosA* and bla_{SHV}). Additionally, biofilm production results varied greatly, likely due to the numerous factors involved in its formation. Surprisingly, mobile strains were found for all three types of motility studied (swimming, swarming, and twitching), despite being considered *K. pneumoniae* a non-motile bacteria. The conjugation of an OXA-48-encoding plasmid was demonstrated in a MDR-hvKp isolate. Infections in *Galleria mellonella* larvae confirmed the high virulence of selected strains, showing the virulence capability of these isolates. These findings suggest that *K. pneumoniae* hypervirulence is multifactorial, involving a complex interplay of genetic and phenotypic factors, which complicates the identification of specific virulence determinants and therefore treatment strategies.

ABBREVIATION GLOSSARY

- ATCC: American Type Culture Collection
- AZ^R: Sodium Azide Resistant
- BFM: Bacterial Flagellar Motor
- cKp: Classical *Klebsiella pneumoniae*
- CV: Crystal Violet
- ESBLs: Extended-Spectrum Beta-Lactamases
- FBS: Fetal Bovine Serum
- FCF: Flow Cell Flush
- FCT: Flow Cell Tether
- GMPc: Cyclic Guanosine Monophosphate
- HS: High Sensitive
- HUMV: Hospital Universitario Marqués de Valdecilla
- hvKp: Hypervirulent *Klebsiella pneumoniae*
- IDIVAL: Instituto de Investigación Valdecilla
- LIB: Library Beads
- LPS: Lipopolysaccharide
- MALDI-TOF: Matrix-Assisted Laser Desorption/Ionization Time-of-Flight Mass Spectrometry
- MDR: Development of multidrug resistance
- MHA: Mueller-Hinton Agar
- MHB: Mueller-Hinton Broth
- MIC: Minimum Inhibitory Concentration
- MLST: Multilocus Sequence Typing
- NGS: Next-Generation Sequencing
- PCR: Polimerase chain reaction
- SB: Sequencing Buffer
- ST: Sequence Type
- UFC: Colony Forming Units
- UTI: Urinary Tract Infection
- WGS: Whole Genome Sequencing

1. INTRODUCTION

1.1 *Klebsiella pneumoniae*

Klebsiella pneumoniae is a capsulated gram-negative enterobacterium that resides in both the environment and abiotic surfaces. It is commonly associated with serious infections such as pneumonia, urinary tract infections (UTIs), and sepsis. Traditionally, *K. pneumoniae* was considered an opportunistic bacterium, mainly responsible for nosocomial infections in immunocompromised patients or those with hospital-related risk factors. However, in recent decades, there has been an alarming increase in the incidence of infections caused by this bacterium, partly due to the emergence of hypervirulent (hvKp) and/or antibiotic-resistant strains, significantly complicating the treatment of these infections (Wyres et al., 2020; Wahl et al., 2024). These hypervirulent strains of *K. pneumoniae* differ from classical strains (cKp) in their ability to cause severe infections in previously healthy individuals. The rapid spread of these hypervirulent and resistant strains poses a serious threat to global health due to their high morbidity and mortality. This threat is reflected in studies such as that of Paczosa et al., 2016 which have documented the increasing impact of these infections in different regions of the world.

Phenotypically, hypervirulent strains of *K. pneumoniae* are known as hypermucoid due to their high viscosity, observable through the String test. An isolate is considered positive in the String Test when touching a colony on an agar plate with a culture loop is so viscous that it extends at least 5 mm from the agar surface. However, this test is presumptive and not confirmatory that the strain is hypervirulent. To consider a strain hypervirulent, molecular characterization using whole genome sequencing (WGS) or via PCR, targeting specific genes associated with hypervirulence in *K. pneumoniae*, are more accurate markers. Some of these genes, present in virulence plasmids or in integrative or conjugative elements studied in this work, are: *ybtA*, *peg-344*, and *rmpA*. These genes contribute to the bacterium's ability to evade the host's immune system and cause severe invasive infections. For example, the *rmpA* gene (regulator of mucoid production) is associated with the production of thicker and more protective capsules, while other genes facilitate the acquisition of essential nutrients such as iron through the production of siderophores.

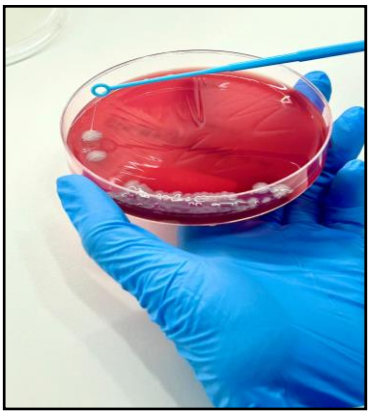

Figure 1. Positive "String test" result.

Furthermore, the majority of hvKp strains belong to a small collection of clonal groups. Multilocus Sequence Typing (MLST) is an essential tool in the study of the epidemiology and evolution of bacterial pathogens, such as hvKp. This approach enables the precise characterization

of bacterial strains by analysing the sequences of multiple loci in the genome, facilitating the identification of specific variants and comparison with other strains on a global scale.

In the context of hypervirulent *K. pneumoniae* (hvKp), the identification of MLST is crucial for understanding the distribution and prevalence of different genetic variants that may be associated with clinical outbreaks, virulence, and antibiotic resistance (Choby et al., 2019). This method not only provides information on the population structure of the strains but also helps in tracking the spread of specific clones and assessing the effectiveness of control and prevention measures.

1.2 Virulence Factors of hvKp

The identification of specific virulence factors of hvKp is crucial for developing effective prevention and therapy strategies. These factors not only explain the ability of these strains to cause severe diseases but also allow us to interfere with their pathogenic mechanisms. As research on hvKp progresses, it has become evident that these strains possess a series of genetic and phenotypic characteristics that distinguish them significantly from the less virulent cKp (Shon et al., 2013). These factors include excessive capsule production, synthesis of potent siderophores, presence of virulence plasmids, and production of various adhesins, toxins, and enzymes that facilitate invasion and tissue damage. (Russo et al., 2019). These factors will be mentioned and explained throughout the report to provide a detailed understanding of how they contribute to the pathogenicity of hvKp.

1.3 Biofilm

One of the most important virulence traits in *K. pneumoniae*, which enables it to colonise the respiratory, gastrointestinal, urinary tracts, and other abiotic surfaces such as catheters, is the ability to form a biofilm. This biofilm is composed of cells adhered to a substrate through an extracellular polymeric matrix formed by polysaccharides, proteins, and DNA. One advantage that this biofilm provides to bacteria such as *K. pneumoniae* is increased resistance to exogenous stressors and antimicrobials. In addition, it allows them to inhibit the immune system by preventing antibodies and antimicrobial peptides from approaching due to their extracellular matrix (Piperaki et al., 2017; Vuotto et al., 2017).

Our bacteria of interest in this study, *K. pneumoniae*, is composed of surface structures that are also involved in biofilm formation. These include, for example, type III fimbriae, which are responsible for substrate adhesion, capsular polysaccharides, which mediate cell-cell communication, iron metabolism, or the presence of different bacterial species through quorum

sensing (Guerra et al., 2022).

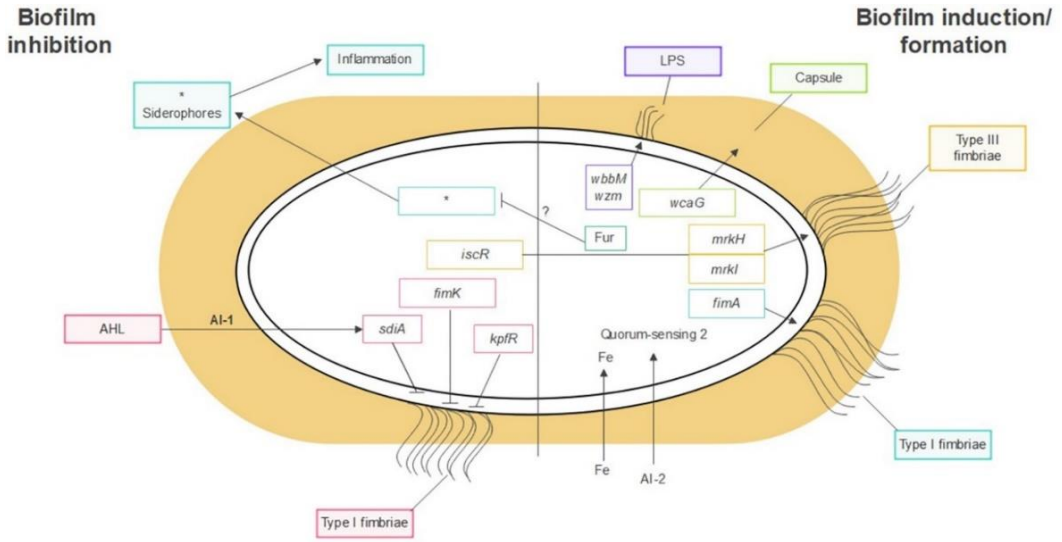

Figure 2. Factors contributing to the formation of *K. pneumoniae* biofilm (Guerra et al., 2022).

Capsular polysaccharides serve as a protective mechanism for the bacterium by inhibiting complement degradation and preventing bacterial opsonization and phagocytosis (Piperaki et al., 2017). Moreover, there is evidence that they are capable of influencing *K. pneumoniae* biofilm formation, particularly in adhesion to surfaces and biofilm maturation. One of the genes investigated in this work was *wcaG,* which is involved in capsule biosynthesis and is associated with increased biofilm formation in *K. pneumoniae* strains causing bacteremia.

Lipopolysaccharide (LPS) is another factor associated with *K. pneumoniae* biofilm formation. Also, it is an essential component in the outer membrane of gram-negative bacteria. It has also been observed to be very important in the initial stages of biofilm formation, especially in adhesion to abiotic surfaces (Balestrino et al., 2008).

Another component of *K. pneumoniae* involved in adhesion to biological and abiotic surfaces are type I and type III fimbriae (Piperaki et al., 2017). Type I fimbriae bind to mannose receptors, while type III fimbriae bind to various cell types *in vitro*, such as those in the lung or bladder. Among these, type III fimbriae are thought to enhance biofilm formation.

Iron metabolism is also involved in the regulation of various virulence factors, including biofilm. Iron deficiency, which bacteria may face when they come into contact with the host, is one of the factors that can trigger infection and colonization. *K. pneumoniae* has four iron uptake systems in which siderophores such as enterobactin, yersiniabactin, salmochelin, and aerobactin act. These siderophores have a high affinity for iron and are one of the strategies used by bacteria to acquire iron from mammalian hosts (Gomes et al., 2020). Aerobactin (*aerobactin*) and yersiniabactin

(*ybtA*) were genes investigated in this work, as they are found in hypervirulent strains of *K. pneumoniae* (Russo et al., 2014; Paczosa et al., 2016).

Finally, the quorum sensing system regulates all phases of biofilm formation (Guilhen et al., 2019; Saxena et al., 2019). This is a mechanism used by bacteria of the same or different species to communicate with each other through the production, secretion, and detection of different molecules known as autoinducers (Balestrino et al., 2005). This system is very useful due to the different environmental stimuli that a bacterium undergoes, requiring rapid adaptation. When bacteria detect a signal that exceeds the threshold, they induce a change in the expression of some genes that alter their phenotype, the expression of virulence factors, or biofilm formation (Balestrino et al., 2005; Saxena et al., 2019).

1.4 Motility

The genus *Klebsiella* is considered to be non-motile and non-flagellated, despite having genes related to motility (*fliC*, *fliA*, and *flgH*) (Carabin-Lima et al., 2016). Motility is also a virulence factor that aids in host tissue colonization. Furthermore, the relationship between migration and chemotaxis helps bacteria to detect nutrient sources. The main organelle for bacterial motility is the flagellum, a supramolecular motility machinery that converts chemical energy obtained from ion flow into mechanical rotation. The flagellum is composed of a bacterial flagellar motor (BFM), a hook serving as a universal joint, and a helical filament acting as a propeller (Kinosita et al., 2023).

Most bacteria exhibit at least one form of motility. In 1972, different types of microbial motility were characterized and named: swarming, swimming, twitching, gliding, sliding, and darting. In this work, we will focus on the first three classes of motility mentioned.

Swimming is employed by bacteria when they encounter unfavorable conditions to ensure survival. In this case, flagellar rotation is used to move in aqueous environments. The direction and regulation of flagellar rotation allow bacteria to move in chemical gradients, known as chemotaxis.

Swarming arises from the differentiation of vegetative cells into cells with a large number of flagella. Its characteristics include the ability to migrate at high speed and in a coordinated manner on solid surfaces. Phenotypes of bacteria in swarming are highly diverse even within the same strain. This type of motility depends on cell density, surface contact, and physiological signals. In addition, this motility requires signals from the quorum sensing system and cyclic GMP network. These signals activate flagellar biogenesis through the main flagellar operon *flhDC*, which is the

most important point in the regulatory network of cellular differentiation and migration for this motility. In gram-negative bacteria, surface detection occurs in two ways: through inhibition of flagellar rotation and/or through detection of contact of the O antigen of LPS with a solid surface. It is also believed that LPS acts as an osmolarity agent facilitating swarming (Zegadło et al., 2023). Compared to swimming, chemotaxis is not necessary in this motility; it relies on flagellar thrust and mechanical interactions. Swarming motility is also closely associated with antibiotic resistance, providing cells with increased nutrient availability and a competitive advantage due to secreted surfactants.

Twitching occurs in some bacteria that produce rapid and random movements of cellular extensions, such as type IV pili or fimbriae. Through these structures, they are able to generate force to glide on solid surfaces or to approach other bacteria. This type of motility is especially important for colonising solid surfaces, such as human tissues or medical devices such as catheters. Furthermore, they can also use this motility to transfer genetic material such as plasmids and DNA.

1.5 Conjugation

Genes conferring antimicrobial resistance can be present in bacterial chromosomes or in extrachromosomal elements such as plasmids. The latter can be horizontally transmitted between bacteria through conjugation, disseminating worldwide and thereby increasing the spread of resistance. The two main types of antibiotic resistance in this bacterium are, on one hand, extended-spectrum β-lactamases (ESBLs), which confer resistance to cephalosporins and monobactams, and on the other hand, carbapenemases, which confer resistance to almost all β-lactams, including carbapenems (Paczosa et al., 2016). Some of the most important carbapenem resistance plasmids, which can be utilized by a wide range of enterobacterial species as hosts, are those that codes for the OXA-48 carbapenemase, such as pOXA-48 EC7215 (Figure 3). Additionally, the virulence of bacteria such as *Escherichia coli* and *K. pneumoniae* has also been associated with the presence of these plasmids (Hamprecht et al., 2019).

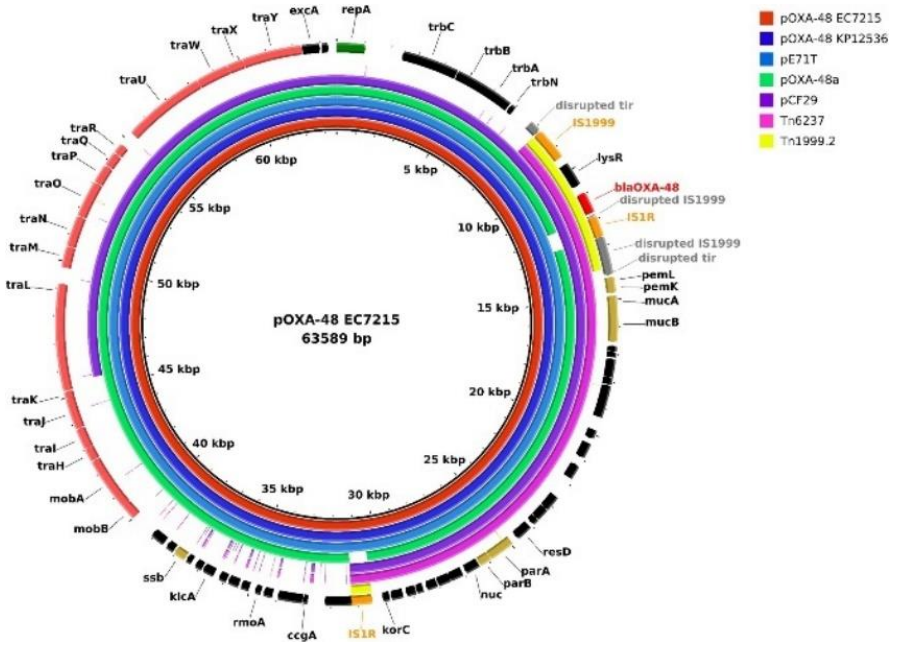

Figure 3. Map of pOXA-48 EC7215, an example of a carbapenamase OXA-48-producing plasmid (Hamprecht et al., 2019).

1.6 Infection assays with *G .mellonella*

The wax moth larva, *Galleria mellonella*, is currently being used as an alternative host infection model due to the limitation of large numbers of mice required to obtain statistically significant results. These larvae have the advantage of being easy to maintain and infect, and they are susceptible to genetic manipulation, allowing aspects of the vertebrate immune response to be modelled after infection. However, a limitation of this model is that it lacks an adaptive immune response, relying solely on the innate immune system, which is responsible for the early elimination of most infections. Besides, *G. mellonella* has a characteristic that distinguishes it from many other invertebrates used to model host-pathogen interactions, which is its ability to grow at 37°C, the optimal temperature for most human pathogens. This is essential because virulence gene expression is often temperature-regulated, which can influence the pathogen's response to hosts (Insua et al., 2013).

In the present study, an exhaustive investigation was conducted to characterize the determinants of resistance and virulence of *K. pneumoniae*. This included: i) characterization using whole-genome sequencing (WGS) to identify virulence and resistance determinants at the molecular level; ii) analysis of biofilm production, which is crucial for antibiotic resistance and persistence of infection; iii) determination of bacterial motility to better understand its dissemination and observe its influence on biofilm; iv) conjugation studies to explore the transfer of antimicrobial resistance genes; v) infection assays using the *G. mellonella* model to study virulence in an invertebrate host system.

2. OBJECTIVES

1. Phenotypic and genotypic characterisation, of hypervirulent *Klebsiella pneumoniae* (hvKkp) isolates collected at the Microbiology Service of Hospital Universitario Marqués de Valdecilla between November 2021 to April 2023.

2. Identify and analyse virulence factors and antimicrobial resistance genes present in hvKp isolates using next-generation sequencing (NGS) techniques such as the MinION platform (Oxford Nanopore).

3. Evaluate the transferability of resistance and virulence plasmids in a representative sample of hvKp isolates through bacterial conjugation studies.

3. MATERIAL AND METHODS

3.1 Study design

The study was conducted at the Microbiology Service of Hospital Universitario Marqués de Valdecilla (HUMV) and at the Instituto de Investigación Valdecilla (IDIVAL). Moreover, some isolates of *K. pneumoniae* from Hospital Universitario Basurto, Hospital de Sierrallana and Hospital Comarcal de Laredo were included. Bacterial isolates were collected between November 2021 to April 2023.

3.2 Study strains

The study included 191 isolates of *K. pneumoniae*, previously identified by MALDI-TOF system (Vitek M, BioMérieux). Of these, 41 isolates were sequenced after PCR screening, and a varying number of strains were selected for each corresponding experiment. The isolates analysed in this study were selected for presenting a hypermucoviscous phenotype (hypermucoid), which is typically associated with the phenomenon of hypervirulence.

3.3 Screening of virulence genes by PCR

The isolates of *K. pneumoniae* initially positive in the string test were subjected to PCR using different combinations of primers designed to amplify some of the most common genes considered biomarkers of hypervirulence in *K. pneumoniae* (Table 1) as described by (Jian-Li et al., 2017). For DNA extraction, we used the InstaGene™ protocol, in which 200 µL of this resin was added to the bacterial sample and resuspended. It was then left in the thermoblock for 20 minutes at 56 ºC, incubated at 100 ºC for 8 minutes, and centrifuged at 10,000 rpm for 10 minutes.

Table 1. Specific primers used for the amplification of target genes in *Klebsiella pneumoniae* (Jian-Li et al., 2017).

TARGET	PRIMER	SEQUENCE (5´-3´)	SIZE (BP)
Capsular type K1	MagAF1	GGTGCTCTTTACATCATTGC	1283
	MagAR1	GCAATGGCCATTTGCGTTAG	
Capsular type K2	K2wzyF1	GACCCGATATTCATACTTGACAGAG	641
	K2wzyR1	CCTGAAGTAAAATCGTAAATAGATGGC	
Capsular type K5	K5wzxF	TGGTAGTGATGCTCGCGA	280
	K5wzxR	CCTGAACCCACCCCAATC	
Capsular type K20	wzyK20F	CGGTGCTACAGTGCATCATT	741
	wzyK20R	GTTATACGATGCTCAGTCGC	

Capsular type K54	wzxK54F	CATTAGCTCAGTGGTTGGCT	881
	wzxK54R	GCTTGACAAACACCATAGCAG	
Capsular type K57	wzyK57F	CTCAGGGCTAGAAGTGTCAT	1037
	wzyK57R	CACTAACCCAGAAAGTCGAG	
rmpA	rmpAF	ACTGGGCTACCTCTGCTTCA	536
	rmpAR	CTTGCATGAGCCATCTTTCA	
aerobactin	aerobactinF	GCATAGGCGGATACGAACAT	556
	aerobactinR	CACAGGGCAATTGCTTACCT	
allS	allsF	CCGAAACATTACGCACCTTT	1090
	allsR	ATCACGAAGAGCCAGGTCAC	
kfuBC	kfuBC-F	GAAGTGACGCTGTTTCTGGC	797
	kfuBC-R	TTTCGTGTGGCCAGTGACTC	
wcaG	wcaG-F	GGTTGGKTCAGCAATCGTA	169
	wcaG-R	ACTATTCCGCCAACTTTTGC	
iucB	iucB-F	ATGTCTAAGGCAAACATCGT	948
	iucB-R	TTACAGACCGACCTCCGTGA	
iroNB	iroNB-F	GGCTACTGATACTTGACTATTC	992
	iroNB-R	CAGGATACAATAGCCCATAG	
ureA	ureA-F	GCTGACTTAAGAGAACGTTATG	337
	urea-R	GATCATGGCGCTACCT(C/T)A	
wabG	wabG-F	CGGACTGGCAGATCCATATC	683
	wabG-R	ACCATCGGCCATTTGATAGA	
uge	uge-F	GATCATCCGGTCTCCCTGTA	535
	uge-R	TCTTCACGCCTTCCTTCACT	
fim	fm-F	TGCTGCTGGGCTGGTCGATG	550
	fm-R	GGGAGGGTGACGGTGACATC	
ybtA	ybtA-F	ATGACGGAGTCACCGCAAAC	960
	ybtA-R	TTACATCACGCGTTTAAAGG	
peg 344	peg 344_F	GCCAGCGTCTATTTCAACTT	102
	peg 344_R	CGGCAAAGTCCTGGGTTTAC	

All PCR reactions were performed in a total volume of 25 µL, using 2 µL of the extracted DNA, 12.5 µL of KAPA2G Fast HotStart ReadyMix (Roche), 1.25 µL of each primer, and 8 µL of nuclease-free water. Isolates of *K. pneumoniae* that presented the target genes were used as positive controls.

3.4 Sequencing

3.4.1 DNA extraction

Genetic material extraction was performed using the DNeasy Blood and Tissue kit (Qiagen,

Hilden, Germany). Each bacterial isolate was resuspended in 200 µL of TE pH8 (10 mM Tris, 1 mM EDTA). Then, 20 µL of proteinase K and 200 µL of buffer AL were added. The mixture was vortexed and incubated for 10 minutes in a thermoblock at 56 ºC. Subsequently, 200 µL of pure ethanol was added, and the entire content was transferred to an extraction column. The column was centrifuged for 3 minutes at 6,000 g. The waste tube was decanted, and the vacuum was reapplied to the column. Then, 500 µL of AW1 was added and centrifuged for 1 minute at 6,000 g. After discarding the waste tube, 500 µL of AW2 was added, and centrifugation was carried out at 14,000 rpm for 5 minutes. The waste tube was again discarded, and centrifugation was performed for 1 minute at 6,000 g, followed by leaving the open columns for 2 minutes to promote alcohol evaporation. Finally, 50 µL of buffer AE was added, left for one minute, and centrifuged again at 6,000 g. The column was discarded, and the entire volume was transferred to a LoBind Eppendorf tube. DNA samples were stored at -20°C until further use.

3.4.2 DNA library preparation for sequencing

The DNA concentration was quantified using a Qubit™ 4 fluorometer (Invitrogen) with 1X dsDNA High Sensitivity (HS) reagent (Invitrogen). Library preparation was performed using the Rapid genomic barcoding kit SQK-RBK114.24 (OxfordNanopore), following the manufacturer's instructions. For this, 50 ng of each bacterial DNA sample was used, and the corresponding barcodes were added. The mixture was incubated in a thermocycler at 30°C for 2 minutes and then at 80°C for 2 minutes. The contents of the tubes were combined in a 1.5 ml LoBind Eppendorf tube, and the same volume of magnetic beads was added. The tube with the mixture was placed on a HULA orbital shaker (Bonsailab) for 5 minutes and then transferred to a magnetic rack for approximately 1 minute until the beads adhered to the tube wall and the supernatant was discarded. 140 µL of 70% ethanol was added and removed immediately, and the procedure was repeated. The tube was placed back on the magnetic rack with the lid open to evaporate the remaining ethanol. Then, 15 µL of Elution Buffer (EB) was added, flicked, and incubated at room temperature for 10 minutes. The tube was again placed on the magnetic rack for one minute to separate the beads, and the entire volume was transferred to a new 1.5 ml LoBind Eppendorf tube. Before loading the Flow Cell, 1 µL of the adapter (RA) was added to the barcodes, incubated for 5 minutes at room temperature, and the priming mix was prepared with 1,170 µL of FCF (Flow Cell Flush), 5 µL of FBS (UltraPure™ BSA 50 mg/ml), and 30 µL of FCT (Flow Cell Tether).

To prepare the Flow Cell, it was first purged to ensure no bubbles remained, and 800 µL of the priming mix was added through the priming port, followed by a 5-minute wait. During this time, the library was prepared in a 1.5 ml LoBind tube by adding 37.5 µL of Sequencing Buffer (SB), 25.5 µL of Library Beads (LIB), and 12 µL of the DNA library. Finally, the Flow Cell was loaded

by opening the SpotON, adding 200 µL of the priming mix through the priming port and 75 µL of the library through the SpotON. Sequencing was performed on a Flow Cell R10.4 and a MinION Mk1C sequencer (OxfordNanopore Technologies) for 24 hours.

Once sequencing was completed, the Flow Cell was washed by adding 2 µL of the wash mix (WMX) and 398 µL of the wash diluent (DIL) into a LoBind tube. Initially, all liquid from the waste port was removed, followed by the addition of 400 µL of the wash mix through the priming port of the Flow Cell. After closing the priming port, a one-hour incubation period ensued, and subsequently, all liquid from waste port 1 was removed once more.

3.4.3 Bioinformatic analysis

The sequencing data were generated in real-time over a period of 24-48 hours using the MinKNOW control software. Initially saved in .fast5 files, containing the sequencer's electrical signal data, they were then converted to fastq format using Guppy software v7.1.4 running on MinKNOW suite v.23.07.12. Long reads were verified and filtered for quality control using NanoPlot v.1.41 and chopper v.0.6.0, discarding reads with less than 250 bp in length or with an average quality below 10, and trimming the first 20 bases at the 5' end. Contamination was excluded by verifying reads with Kraken2. Long read assembly was performed using Flye 2.9.2-b1786, polished with medaka v.1.8.0, and their starting positions were set at the *recA* gene with circlator v.1.5.5 for more convenient chromosome alignment and comparison. Assemblies were quality-checked using Quast v.5.2.0 and annotated with Bakta v.1.7.0. The presence of plasmids and integrons was verified using MOB suite v.3.0.3, copla v.1.0, and integron_finder v.2.0, respectively. Antimicrobial resistance (AMR) and virulence genes were detected using abricate v.1.0.1 and ResFinder/VFDB databases, respectively.

3.5 Biofilm quantification

Quantitative estimation of biofilm formation was performed in 24-well plates using the method described by O'Toole et al., 1998, with some modifications.

The study strains were streaked on blood agar plates and then incubated in a 37°C incubator overnight.

The following day, dilutions of each bacterial isolate were prepared in 3 ml of sterile saline, adjusting the optical densities to 3 McFarland units using a spectrophotometer. Twenty-four-well plates were prepared with 900 µL of Mueller-Hinton broth (MHB) in each well, followed by the

addition of 100 µL of the previously adjusted cultures. Three wells in each plate were left uninoculated in each plate to serve as negative controls, subtracting this value from the rest of the strains in that same biological replicate. Each bacterial isolate was inoculated into three wells to have three technical replicates, and the experiment was repeated on three different days to obtain three biological replicates. The plates were then incubated for 24 h at 37°C.

After 24 hours, the plates were removed from the incubator, and the culture medium from all wells was discarded using a pipette. Each well was washed three times with 1 ml of Milli-Q water to remove any remaining planktonic cells. Once all the residual water in the wells was removed, the plates were allowed to air dry for approximately 20 minutes at room temperature. For biofilm staining, 1 ml of Crystal Violet (CV; 0.7% w/v; Sigma, prepared with Milli-Q water) was added to each well and left for 12 minutes at room temperature. Subsequently, the CV was removed with a pipette, and the plates were washed three times with Milli-Q water to remove excess dye, followed by air drying for at least 30 minutes.

To measure biofilm production, the CV was solubilized with 1 ml per well of a 33% acetic acid solution. Plates were placed on a shaker for 5-10 minutes before reading to ensure CV solubilization. Biofilm quantification was performed using a NanoQuant Infinite M200 PRO plate reader (TECAN) at an optical density of 595 nm with prior shaking for 20 seconds. Nine measurements were taken from each well, and the mean was calculated, discarding any outliers or highly dispersed values to obtain a more representative and homogeneous data set.

3.6 Motility

On the first day, all study strains and controls were inoculated onto blood agar plates. *Pseudomonas aeruginosa* ATCC 27853 was used as a positive control, while *K. quasipneumoniae* ATCC 700603 served as the negative control. Additionally, a strain of *Proteus mirabilis* 4354195 was used as a positive control for motility, along with *P. aeruginosa* PAO1 and PA14.

The medium was prepared on the same day as the experiment. The composition of the medium for 400 ml was as follows:

- Peptone: 4g
- NaCl: 2.4g
- Agar: 1g. The agar concentration varied depending on the type of motility: For swimming, the proportion was 0.25%, for swarming 0.5%, and for twitching 1%.
- Beef extract: 1.2g.

- 2.3.5-Triphenyltetrazolium: 20mg

The medium was autoclaved and plated, allowing it to dry in a laminar flow hood for exactly 20 minutes. Before inoculating the strains, it was necessary to adjust the optical density to 0.2 McFarland in Mueller-Hinton broth (MHB). Once all strains reached the same optical density, 2 µL were inoculated onto the corresponding plates using a pipette. The procedure varied depending on the type of motility: for swimming, the pipette tip was inserted halfway into the agar width; for swarming, it was inoculated onto the surface; and for twitching, the pipette tip was inserted to the bottom of the agar. Plates were then incubated in a 37°C incubator for 20 hours, covered with a bag to prevent medium desiccation.

On the third day, the plates were observed, and the diameter (cm) of the halos for each strain was measured. The procedure was repeated on 3 different days under the same conditions.

3.7 Conjugation

To perform conjugation, 3 donor strains were selected from the *K. pneumoniae* strains sequenced in this study, and 1 recipient strain, which in this case was *E. coli* J53 sodium azide resistant (AZ^R).

Our selected donor strains harbored the following plasmids of interest: pOXA-48-Kp754209, pCTX-M-15-Kp943123, pOXA-48-Kp967964 y pCTX-M-15-Kp967964.

On the first day, 7 Falcon tubes were prepared with 5 ml of Mueller-Hinton Broth (MHB) each. Three of them were inoculated with a colony of each donor strain, three with two colonies of the same recipient strain, and the last one was not inoculated with any colony and used as a negative control. The cultures were incubated overnight at 37°C with agitation.

The next day, the cultures were refreshed. For this, seven 150 ml polypropylene flasks were prepared with 20 ml of MHB, and 200 µL of the corresponding culture were added to each one. The cultures were incubated at 37°C with agitation, and the absorbance was measured with a spectrophotometer every two hours approximately, until reaching an optical density of 0.6 at a wavelength of 600 nm. The remaining volume was then distributed into different Eppendorf tubes and centrifuged at 6,000 g for 20 minutes. Subsequently, the maximum volume of supernatant possible was removed, and all pellets were resuspended in one tube and centrifuged again at 6,000 g for 20 minutes, discarding the supernatant. The pellets of the donor and recipient strains were resuspended in an approximate volume of 100 µL, and the conjugation mixture was plated on 3 Mueller Hinton agar (MHA) plates and incubated in an incubator at 37°C overnight.

On the third day, serial dilutions of the conjugation mixture (10^{-1} to 10^{-7}) were prepared, and they

were plated on MHA plates supplemented with the corresponding antibiotics for the selection of transconjugants. For this, the necessary antibiotics were prepared, taking into account their initial concentration and purity.

$$\textbf{Final concentration} = \frac{\textbf{Initial concentrationl}}{\textbf{Purity}}$$

- **Fosfomycin**: 5,483.27 µg diluted in 1 ml of water.

$$\frac{\mathbf{4096\ \mu g}}{\mathbf{74.7/100}} = \mathbf{5,483.27\ \mu g}$$

- **Ampicillin**: 100.00 µg diluted in 1 ml of water.

$$\frac{\mathbf{100.00\ \mu g}}{\mathbf{100/100}} = \mathbf{100.00\ \mu g}$$

- **Ceftazidime**: 4,847.33 µg diluted in 1 ml of water.

$$\frac{\mathbf{4096\ \mu g}}{\mathbf{84.5/100}} = \mathbf{4,847.33\ \mu g}$$

- **Imipinem**: 4,162.60 µg diluted in 1 ml of Phosphate buffer at pH 7.2 y 0.01 M.

$$\frac{\mathbf{4096\ \mu g}}{\mathbf{98.4/100}} = \mathbf{4,162.69\ \mu g}$$

- **Sodium azide**: 100.00 µg diluted in 1 ml of water.

$$\frac{\mathbf{100.00\ \mu g}}{\mathbf{100/100}} = \mathbf{100.00}\ \mu g$$

The agar Mueller Hinton (MHA) plates were prepared with the selected concentrations of antibiotics for each strain, distinguishing between plates for donor strains as controls and those for transconjugants. The plates were prepared in a laminar flow hood and allowed to dry for 20 minutes. For the donor strains, 4 plates were inoculated with dilutions of 10^{-4}, 10^{-5}, 10^{-6} and 10^{-7}, while for the transconjugants, 4 plates were selected with the following dilutions: 10^{-1}, 10^{-2}, 10^{-3} and 10^{-4}.

- 754209
    - **Transconjugants**
        - Sodium Azide: 150 µg/ml
        - Ampicillin : 100 µg/ml
    - **Donors**
        - Imipinem 1 µg/ml
        - Ampicillin 50 µg/ml

- 943123
    - **Transconjugants**
        - Sodium Azide: 150 µg/ml
        - Ceftazidime: 100 µg/ml
    - **Donors**
        - Fosfomycin : 8 µg/ml

- 967964
    - **Transconjugants 1**
        - Sodium Azide: 150 µg/ml
        - Ampicillin : 100 µg/ml
    - **Transconjugants 2**
        - Sodium Azide: 150 µg/ml
        - Ceftazidime: 4 µg/ml
    - **Donors**
        - Fosfomycin : 8 µg/ml

100 µL of each dilution were inoculated onto their respective plate and spread with a Drigalsky loop. The cultures were then incubated overnight 37°C t. On the final day of this procedure, the colonies on each plate were counted, and the following calculations were performed.

$$\textbf{Conjugation frequency (C. F)} = \frac{\textbf{Transconjugants}}{\textbf{Donors}}$$

$$\textbf{UFC/mL} = \frac{\textbf{Nº colonies} \times \textbf{Dilution Factor}}{\textbf{Volume plated}}$$

3.8 Infection assays with *G .mellonella*

In the study of *G. mellonella* infection with hypervirulent *K. pneumoniae*, a selection of strains was made based on identified virulence and resistance genes to evaluate their in vivo virulence. Six isolates were chosen, including 3 from the conjugation study: 754209 (bla_{OXA-48}), 943123 ($bla_{CTX-M-15}$), and 967964 (bla_{OXA-48} and $bla_{CTX-M-15}$), and 3 other isolates: 50124763, 56523365, and Basurto 9. Additionally, two positive controls and two negative controls were included to compare the effects of infection. The positive controls were PAO1, known for its high virulence and rapid killing capacity in these invertebrate hosts, and *E. coli* ATCC 25922, which has a slower mortality rate compared to PAO1. Negative controls consisted of untreated larvae to assess natural mortality and larvae pricked with saline solution to evaluate the effect of the injection procedure without the presence of bacteria.

G. mellonella larvae were acquired from Harkito Reptile (Madrid, Spain) and stored at 8–10°C in darkness on wood shavings, being used for infection within 10 days of receipt. Larvae were selected to have a length of 20–30 mm, presenting a healthy creamy colour without spots or gray marks. Prior to inoculation, *K. pneumoniae* isolates were plated on blood agar plates and incubated overnight in the 37°C incubator. Bacterial cultures were normalized using a 0.5 McFarland standard, and colony-forming units (CFU/ml) were confirmed by viable count assay through serial dilutions from 10^{-2} to 10^{-5}.

To infect the larvae, they were held with sterile forceps. They were disinfected with 70% alcohol using a swab, and 10 µL of the corresponding dilution of each bacterial isolate was injected into the last right proleg. The procedure was performed using a 0.5 ml BD micro-fine syringe. The number of larvae inoculated with each study strain was 30 for the first replicate, and 10 were used for each chosen concentration of 10^3, 10^4, and 10^5. Three replicates were performed for each strain, and after the first replicate, the bacterial concentration with the highest lethal dose was

selected. In this case, all strains were inoculated at a concentration of 10^5 except for PAO1, which, due to its high mortality, was inoculated at 10^4. Larvae were kept in a 37°C incubator in petri dishes, separated by strains and concentrations. Larvae were examined approximately every 2-4 hours for 3 days, and the surviving larvae were recorded at each measurement. Larvae were considered dead when they showed complete melanization and/or did not respond to physical stimuli.

4. RESULTS

4.1 Sequencing

The presence of virulence genes was studied in 41 strains of *K. pneumoniae*. Figure 4 displays the results, with a heatmap constructed from a data matrix where each row represents a strain and each column represents a virulence gene. Binary values (1 for positive and 0 for negative) indicate the presence or absence of each gene.

The data reveal the prevalence of several virulence genes in *K. pneumoniae*. Among the most common are *wabG*, *ureA*, and *fim*, with a prevalence of 92.68% (38 out of 41). Another highly prevalent gene was *uge*, present in 82.92% (34 out of 41) of the strains, followed by aerobactin and *ybtA*, both with a prevalence of 78.04% (32 out of 41). On the other hand, *kfuBC* showed a prevalence of 51.21% (21 out of 41).

Regarding capsular type genes, the most frequent were *magA* (K1) and *wzy_K2* with a prevalence of 24.39% (10 out of 41) and 31.70% (13 out of 41), respectively. In contrast, the presence of *wzx_K5* was not detected in the analysed strains, and *wzy_K20* was observed with a low prevalence of 2.44% (1 out of 41). The genes *wzx_K54* and *wzy_K57* are relatively rare, with a prevalence of 4.87% each (2 out of 41).

In the case of the *peg-344* gene (*), its prevalence of 9.75% (4 out of 41) should be interpreted with caution, as it was not measured in all strains. Initially, this gene was not included in the analysis, but after discovering its importance for the virulence of *K. pneumoniae*, it began to be considered in subsequent strains.

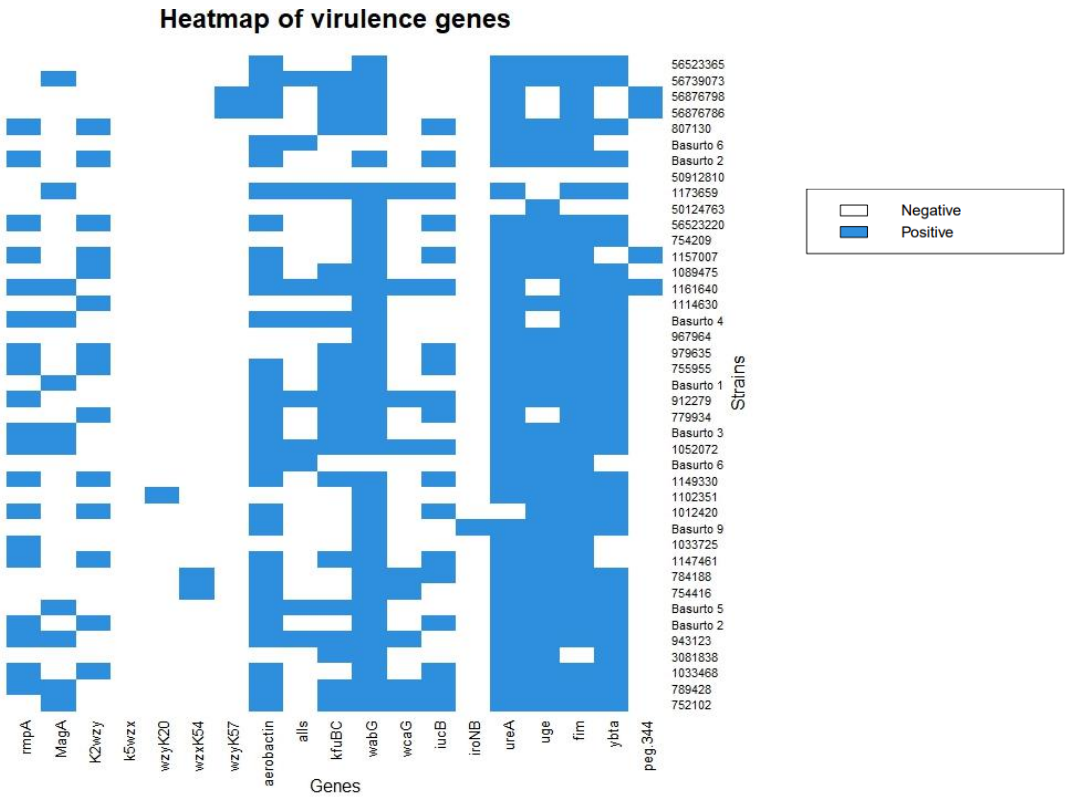

Figure 4. Heatmap showing the presence/absence of virulence genes in different isolates of hypervirulent *K. pneumoniae* analysed in this study. Blue colour indicates presence, while white indicates absence.

The heatmap (Figure 5) generated in our study shows the presence and absence of various antibiotic resistance genes in hypervirulent strains of *K. pneumoniae*. The most prevalent genes in this study, found in 100% of the 34 studied strains, are *oqxA*/*B* and *oqxB* (34 out of 34). The following were *fosA* and bla_{SHV} (in their different allelic variants), present in 94.11% (32 out of 34) and 79.41% (27 out of 34) respectively. The $bla_{\text{SHV-190}}$ variant was the most prevalent, accounting for 28.57% (12 out of 34). Additionally, two of the most discussed resistance genes in this study are $bla_{\text{OXA-48}}$ and $bla_{\text{CTX-M-15}}$, both of which were much less prevalent, present in 8.82% (3 out of 34) and 11.76% (4 out of 34) respectively.

Table 2. Most prevalent allelic variants of bla_{SHV} in hypervirulent *K. pneumoniae* strains in this study.

Allele	Percentage (%)
$bla_{\text{SHV-190}}$	28.57%
$bla_{\text{SHV-1}}$	23.80%
$bla_{\text{SHV-207}}$	14.29%
$bla_{\text{SHV-145}}$	9.52%
$bla_{\text{SHV-187}}$	7.14%

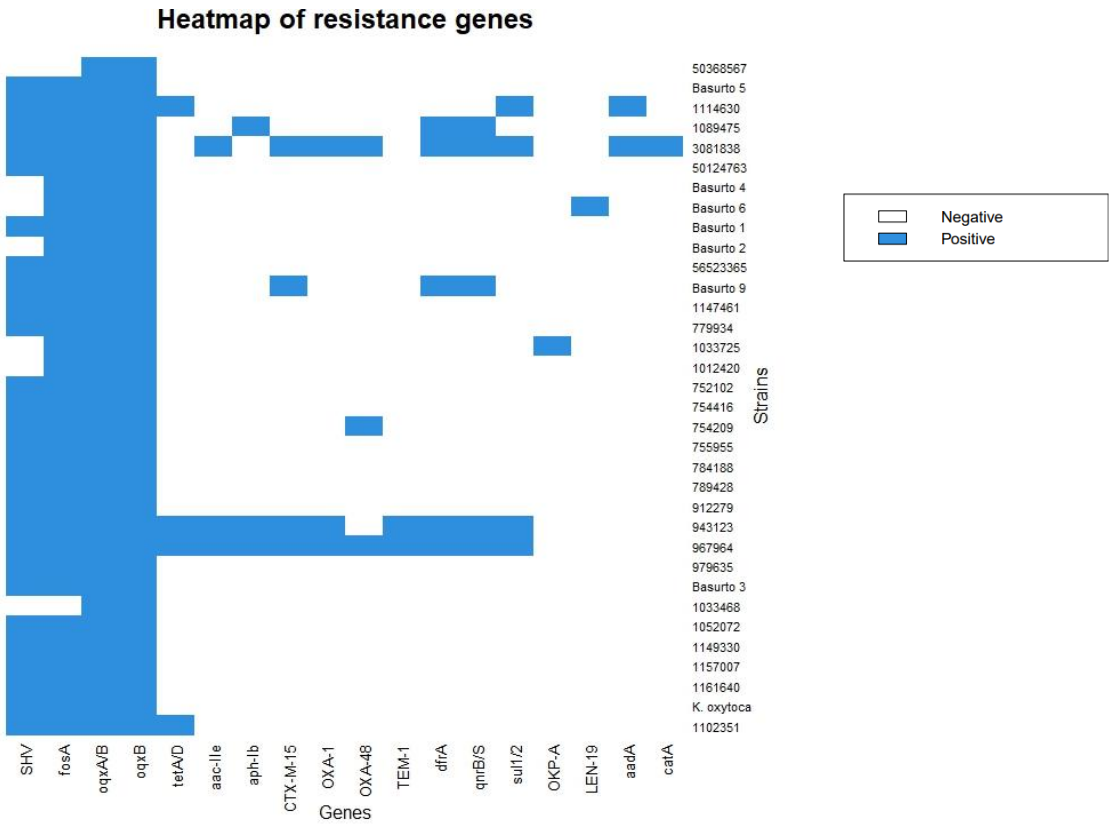

Figure 5. Heatmap showing the presence/absence of resistance genes in different isolates of hypervirulent *K. pneumoniae* analysed in this study. Blue colour indicates presence, while white indicates absence.

In this study, we analysed 41 strains of hypervirulent *K. pneumoniae* to determine their MLST. The results obtained are presented in Table 3, highlighting several MLST types with different frequencies. The most frequent MLST was ST23, present in 21.95% (9 out of 41 strains) of the strains, followed by ST380, with a prevalence of 9.75% (4 out of 41). Other significant MLST types include ST66 and ST198, each with a frequency of 7.31% (3 out of 41).

Table 3. Distribution of the most prevalent MLST types in the study strains of hypervirulent *K. pneumoniae.*

MLST	Percentage (%)
23	21.28%
380	9.52%
66	7.14%
198	7.14%
1805	4.76%
449	4.76%
307	4.76%
714	4.76%
412	4.76%
86	2.38%

4.2 Biofilm Quantification

In this work, the biofilm production of the 191 *K. pneumoniae* isolates was quantified, although for Figure 6, those that had been sequenced and some others with low standard deviation were selected. In total, 57 *K. pneumoniae* strains are represented in the graph as a sample of all those studied. Figure 6 represents the absorbance measured at a wavelength of 600 nm, following the protocol described in Materials and Methods. Despite all strains in this study being considered hypermucoid and hypervirulent, we can observe significant variation in biofilm production among them.

To classify the strains studied as non-biofilm producers, weak, moderate, and strong biofilm producers, a range of optical densities of solubilized biofilm was established based on the article published by Díaz Ríos et al., 2021. Strains with an optical density below 0.05 were classified as non-biofilm producers, those between 0.05 and 0.1 as weak producers, those between 0.1 and 0.3 as moderate producers, and finally, those with an optical density of more than 0.3 were classified as strongly biofilm producers. Therefore, the non-biofilm-producing strains were 11 out of 57 (19.30%), the weak producers were 8 out of 57 (14.04%), the moderate producers were 18 out of 57 (31.58%), and the strongly biofilm producers were 20 out of 57 (35.09%).

Table 3. Classification range of strains according to their biofilm production measured by absorbance at a wavelength of 600nm.

BIOFILM PRODUCTION	Range	N.º of strains	Percentage (%)
Non-producer	< 0.05	11	19.30%
Weak producer	0.05 – 0.1	8	14.04%
Moderate producer	0.1 – 0.3	18	31.58%
Strong producer	> 0.3	20	35.09%

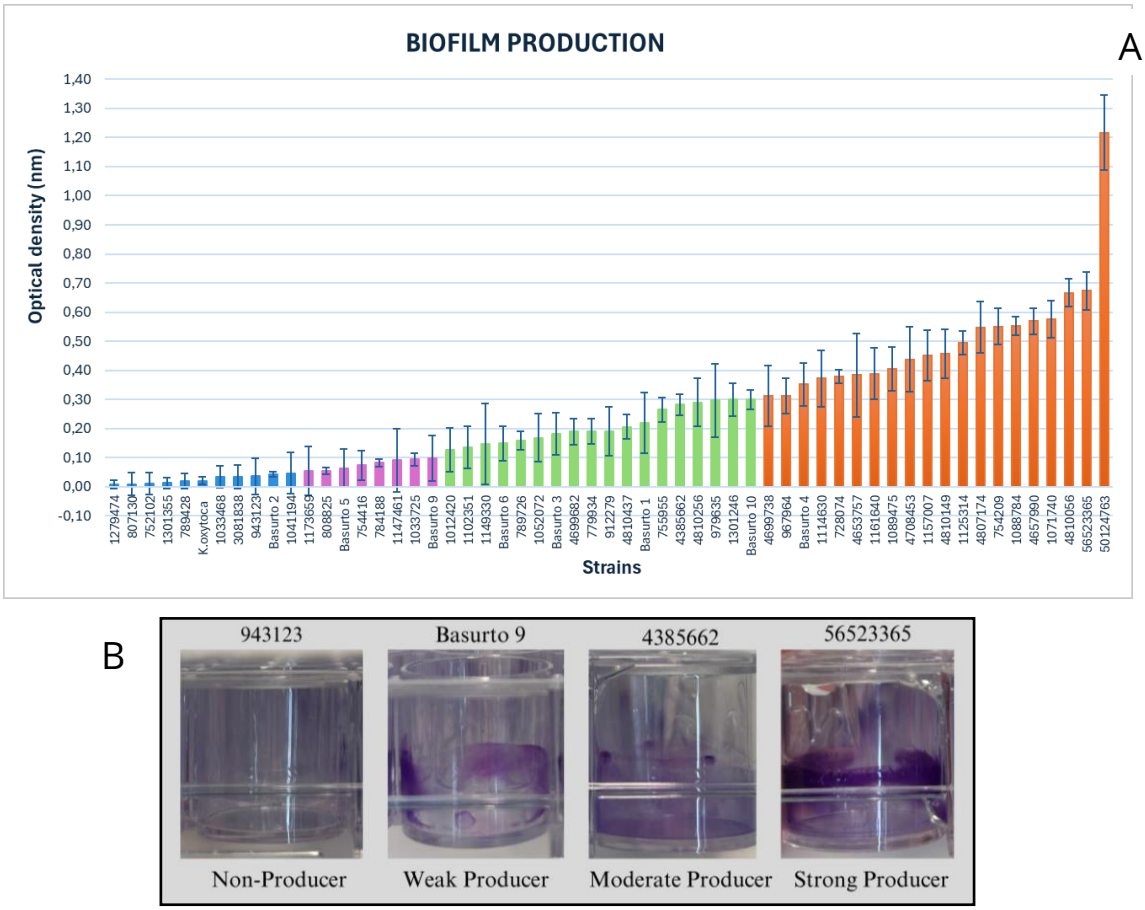

Figure 6. (A) Quantification of biofilm production in hypervirulent and hypermucoid strains of *K. pneumoniae*. The "Y" axis represents absorbance measured at a wavelength of 600 nm, while the "X" axis denotes the numbers of different strains. (B) Images of wells stained with crystal violet showing biofilm formation of various strains.

4.3 Motility

In this study, the swimming, swarming, and twitching motility of the 43 isolates, whose complete genomes were sequenced, was evaluated. To determine if the isolates were mobile or non-mobile, the diameter measurement of the halos of each strain was divided by the diameter measurement of the negative control halo (*K. quasipneumoniae* ATCC 700603) to establish a motility ratio. Isolates were considered mobile when this ratio was greater than 1.5 and non-mobile when it was lower than that value.

In Figure 7A, we can observe that out of the 43 isolates, only 2 (4.6%) were considered non-mobile on swimming plates. Therefore, we found highly mobile bacteria with a significant difference compared to the negative control, with some even surpassing the positive control of *P. aeruginosa* ATCC 27853.

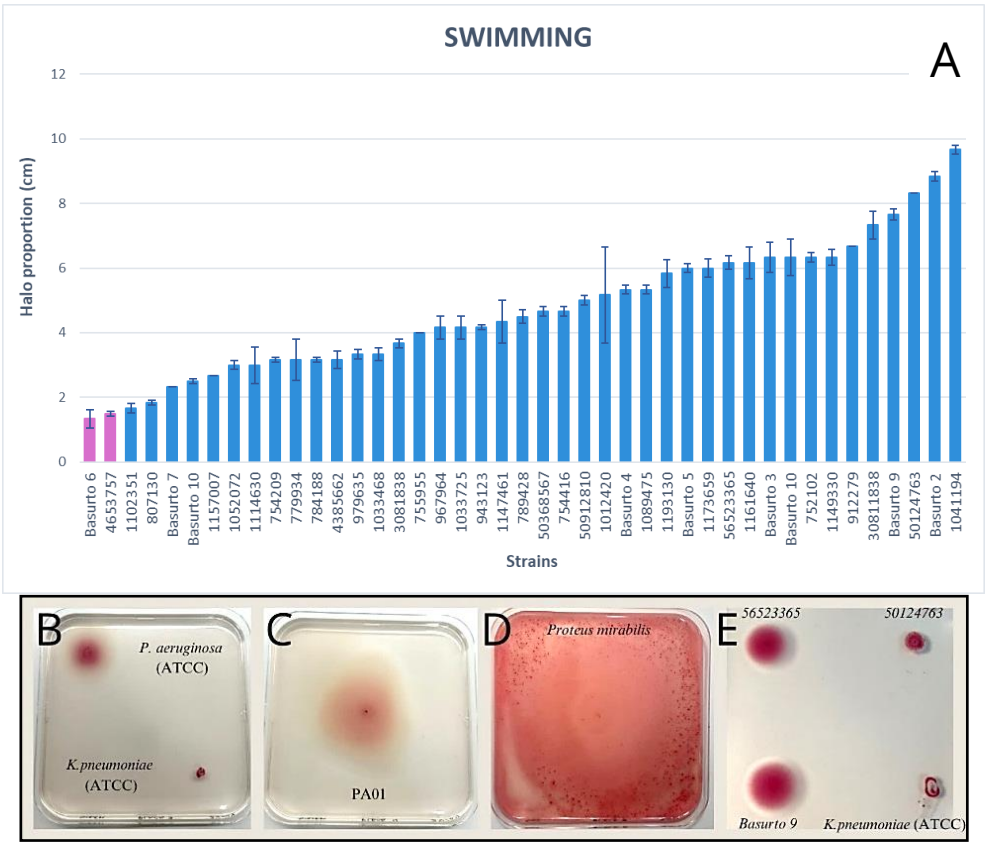

Figure 7. Swimming motility graph of *K. pneumoniae* (A). Images of swimming motility, in the first image, we find the controls used, *P. aeruginosa* ATCC 27853 as the positive control, and *K. quasipneumoniae* ATCC 700603 as the negative control (B), PAO1 (C), Proteus mirabilis 4354195, and three of the studied strains with the negative control as reference (D).

In the case of swarming (Figure 8), 17 isolates were considered non-motile (39.53%) out of the total 43. Compared to the other types of motility, Swarming is where we found the most non-motile bacteria.

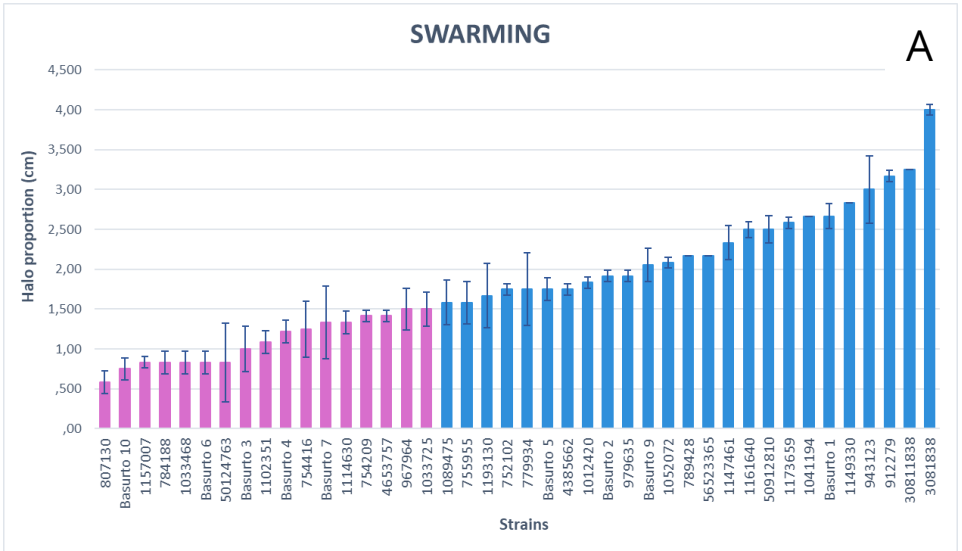

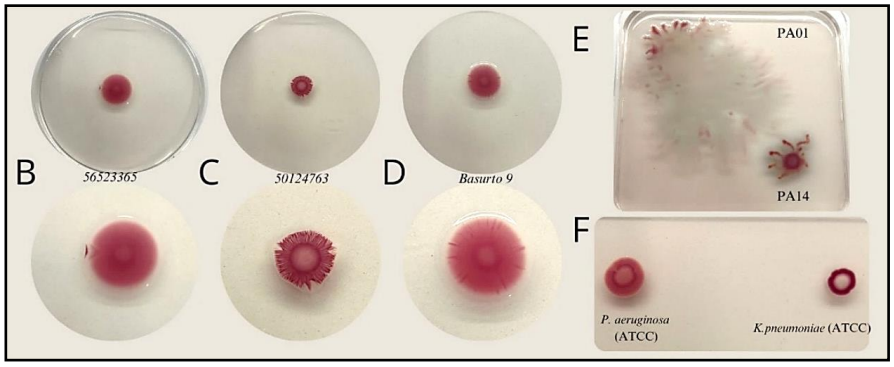

Figure 8. Swarming motility graph of *K. pneumoniae* (A). Images of swarming motility of three strains studied in this work (B, C, and D), PAO1 and PA14 (E), and the controls used, *P. aeruginosa* ATCC 27853 as positive control and *K. quasipneumoniae* ATCC 700603 as negative control (F).

In the case of twitching (Figure 9), 5 isolates were considered non-motile (11.63%) out of the total 43. To measure this type of motility, instead of measuring the upper halo as in the previous cases, the halo at the bottom of the agar was measured.

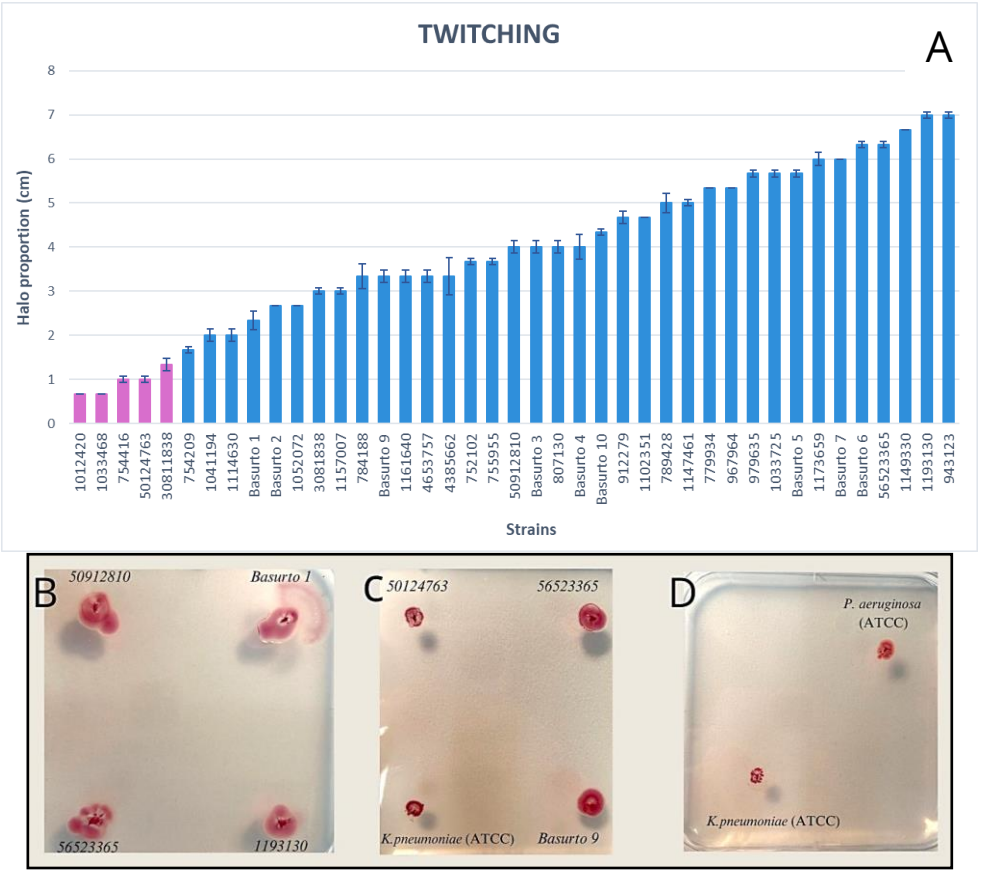

Figure 9. Twitching motility of *K. pneumoniae* (A). Images showing twitching motility of strains studied in this work (B and C) and the controls used: *P. aeruginosa* ATCC 27853 as positive control and *K. quasipneumoniae* ATCC 700603 as negative control (D).

4.4 Conjugation

In the conjugation study between *K. pneumoniae* and *E. coli* J53 AZ^R, successful plasmid transfer was observed in only one of the three selected donor strains in this study (*K. pneumoniae* 754209). The results were obtained by counting plates with transconjugant colonies and plates with donor colonies. The conjugation frequency was calculated using the formula described in the materials and methods section, resulting in a frequency of 8.65 x 10^{-2} (Table 4).

Table 4. Colony Counts and Conjugation Frequency of the plasmid pOXA-48-Kp754209.

754209	**Colonies**	**UFC/ml**	**Average of D y TC**	**Conjugation Frequency**
Donor -7	8	8×10^8	6.18×10^8	$\mathbf{8.65 \times 10^{-2}}$
Donor -6	58	5.8×10^8		
Donor -5	475	4.75×10^8		
Transconjugant -4	315	3.15×10^7	5.35×10^7	
Transconjugant -5	59	5.9×10^7		
Transconjugant -6	7	7×10^7		

Also, to confirm that the resulting strains had indeed conjugated, identification was performed using MALDI-TOF Vitek MS, which revealed that they were *E. coli*, consistent with the transconjugant strain *E. coli* J53 with the plasmid pOXA-48-Kp754209. Furthermore, 11 colonies were selected from one of the transconjugant plates, and PCR was performed to detect OXA-48 (785-798 pb) (Figure 10). As shown in the image, 10 out of the 11 colonies tested positive. Two positive controls are also visible: the first (C+r) is the routine hospital positive control, and the second (C+) which appears fainter, represents our donor strain 754209.

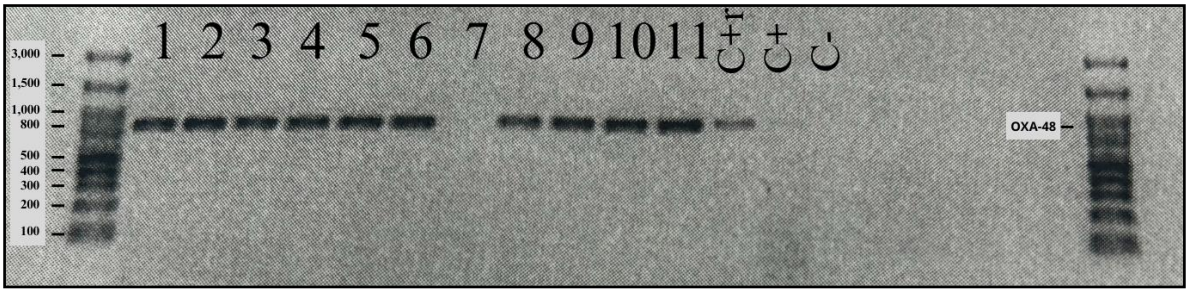

Figure 10. PCR of positive transconjugant colonies for OXA-48. It shows 11 colonies selected from the transconjugant plates, 2 positive controls, one from the routine hospital and the other from the donor strain *K. pneumoniae* 754209 (C+r and C+), and one negative control (C-).

Finally, an antibiogram of the resulting transconjugant colonies was performed and compared with the recipient strain (*E. coli* J53) and the donor strain (*K. pneumoniae* 754209).

Table 5. Comparison of the antibiograms of the transconjugant, recipient, and donor strains of *K. pneumoniae* 754209.

Antibiotics	***TcE. coli* J53(754209)**		***E. coli* J53**		***K. pneumoniae* 754209**	
	CMI	Interpretation	CMI	Interpretation	CMI	Interpretation
Temocillin	>=32	R				
Ampicillin	>=32	R	8	S		
Amoxicillin					>=32	R
Amoxicillin/Clavulanic Acid		R			>=32	R
Piperacillin/Tazobactam	>=128	R	<=4	S	-	-
Cefuroxime	32	R	8	S	4	S
Cefoxitin	<=4	S	<=4	S	<=4	S
Cefixime	0.5	S			-	-
Cefotaxime	<=0,25	S	<=0.25	S	<=1	S
Ceftazidime	<=0,12	S	<=0.12	S	<=1	S
+ Ceftriaxone		S		S	-	-
Cefepime					<=1	S
Ceftazidime/Avibactam	<=0.12	S			0.5	S
Ceftolozane/Tazobactam	<=0.25	S				
Aztreonam	<=1	S			-	-
Ertapenem	0,5	S	<=0.12	S	4	R
Imipenem	2	S			4	I
Meropenem	2	S	<=0.25	S	4	R
Meropenem/Vaborbactam	2	S				
Amikacin	<=1	S	2	S	<=2	S
Gentamicin	<=1	S	<=1	S	<=1	S
Tobramycin	<=1	S			-	S
Nalidixic Acid	<=2	S				
Ciprofloxacin	<=0.06	S	<=0.06	S	<=0.25	R
Minocycline	1	S				
Tigecycline	<=0,5	S			<=0.5	R
Fosfomycin	<=16	S	<=16	S	-	S
Nitrofurantoin	<=0.16	S	<=16	S		
Colistin	0.5	S			2	R
Trimethoprim/Sulfamethoxazole	<=20	S	<=20	S	<=20	R
Description	**OXA-48**		**AZ^{R}**			

4.5 Infection assays with *G. mellonella*

In the *G. mellonella* infection study with hypervirulent strains of *K. pneumoniae*, six different strains were evaluated, three of which were the same as those used in the conjugation assays: 754209 (*bla*$_{\text{OXA-48}}$), 943123 (*bla*$_{\text{CTX-M-15}}$), and 967964 (*bla*$_{\text{OXA-48}}$ and *bla*$_{\text{CTX-M-15}}$). Furthermore, three isolates were considered particularly interesting as they belonged to the same patient over a period of 9 months: 56523365, Basurto 9, and 50124763. Strain 56523365 belonged to the first episode, which was treated with 8 days of IV piperacillin/tazobactam, insufficient treatment leading to a second episode represented by the second isolate, Basurto 9. In this case, the first

abscesses appeared, and percutaneous drainage was performed. Four weeks of IV treatment with piperacillin/tazobactam and ceftriaxone were administered. Finally, the third episode involved the appearance of second abscesses, and percutaneous drainage was repeated. This time, treatment comprised seven days of IV piperacillin/tazobactam and five days of oral ciprofloxacin, considering that in this last episode, the existing subpopulations were the most resistant. These three strains also tested positive in the sequencing for an uncommon capsular type, K30. Additionally, two positive controls and two negative controls were included to compare the effects of infection. The positive controls were PAO1, known for its high virulence and rapid ability to kill these invertebrate hosts, and *E. coli* ATCC 25922, which exhibits a slower mortality rate compared to PAO1. The negative controls consisted of untreated larvae to assess natural mortality and larvae pricked with saline solution (PBS) to evaluate the effect of the injection procedure.

Before performing the procedure outlined in the materials and methods, we conducted a CFU/ml count to determine the bacterial concentration of our strains and whether it corresponded to an optical density of 0.5 McFarland. In Table 6, we can observe that all strains except *E. coli* ATCC 25922 were within the same order of magnitude 10^7.

Table 6. UFC/ml counts of each strain, including the 6 study strains and the two positive controls *E. coli* ATCC 25922 and PAO1.

STRAINS	UFC/ml
50124763	1.13×10^7
56523365	1.65×10^7
Basurto 9	3.39×10^7
943123	1.50×10^7
754209	1.75×10^7
967964	1.37×10^7
***E.coli* ATCC 25922**	4.38×10^6
PAO1	1.25×10^7

The Kaplan-Meier survival curve (Figure 11) depicts the probability of survival of *G. mellonella* larvae over time for each of the strains and controls. The curve reflects differences in larval survival, highlighting the high virulence of *K. pneumoniae* strains compared to positive and negative controls. The negative controls (unpunctured and inoculated with saline solution) showed a high probability of survival over time, around 80% after 72 hours post-infection. In contrast, larvae infected with PAO1 exhibited the highest mortality rate (100% in less than 24 hours), while those infected with *E. coli* ATCC 25922 showed a lower and slower mortality rate, approximately 60% survival after 72 hours from inoculation. Among our study strains, those with the lowest survival rate, less than 50%, were inoculated with *K. pneumoniae* isolates 56523365

and 754209 (bla_{OXA-48}). Conversely, those with the highest survival rate, around 70%, similar to the negative controls, were inoculated with *K. pneumoniae* isolates Basurto 9 and 943123 ($bla_{CTX-M-15}$).

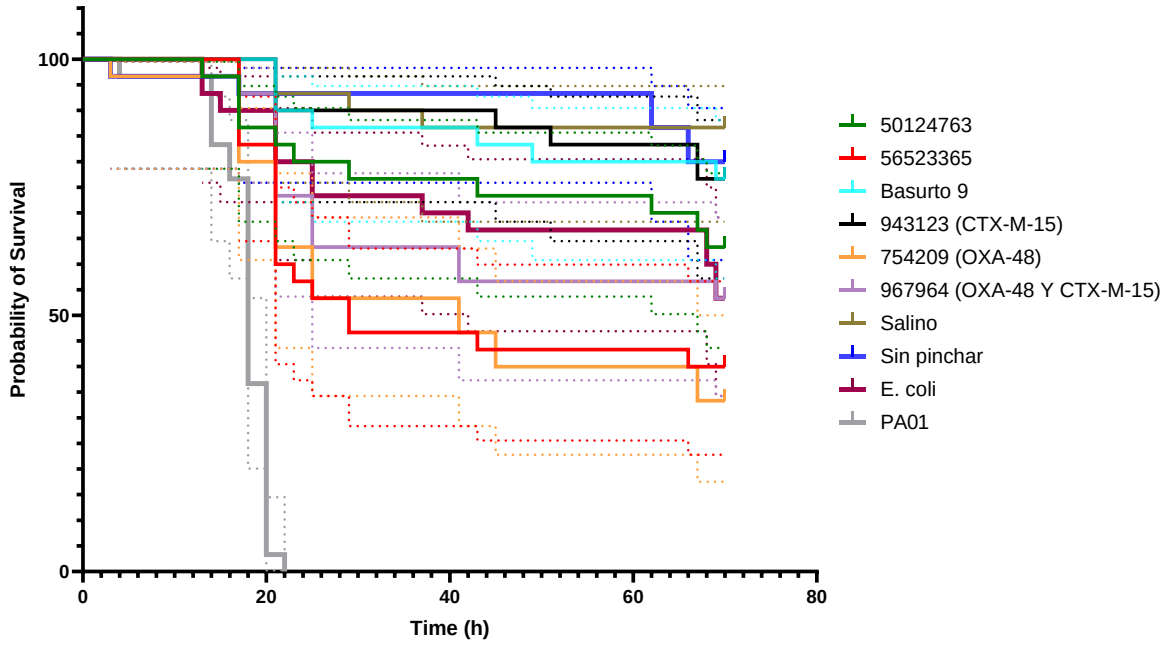

Figure 11. Kaplan-Meier survival curve for *G. mellonella* larvae infected with hypervirulent strains of *K. pneumoniae*. Negative controls included unpunctured larvae and larvae inoculated only with saline solution, while PAO1 was used as a positive control for its high mortality rate, and *E. coli* ATCC 25922 for its mortality, albeit over a longer period of time.

The survival curves revealed significant variations depending on the infecting strain. The Log-rank test (Mantel-Cox) was used to compare the curves between different groups. This analysis yielded a chi-square value of 208.8 with 9 degrees of freedom and a p-value < 0.0001, indicating highly significant differences between the survival curves of the different *K. pneumoniae* strains and the controls. These findings suggest a considerable impact of the infecting strain on the survival of *G. mellonella* larvae. In addition, the Gehan-Breslow-Wilcoxon test, which gives more weight to early survival time events, also showed significant differences between the survival curves, with a chi-square value of 189.6 and a p-value < 0.0001, highlighting the relevance of differences in survival among *K. pneumoniae* strains, especially in the early stages of infection. Furthermore, the Logrank test for trend was used to detect patterns in the survival curves. A significant trend was observed, with a chi-square value of 10.70 and a p-value of 0.0011, suggesting a relationship between the infecting strain and the probability of larval survival.

Table 7. Kaplan-Meier Survival Curve Statistics Results for *G. mellonella* Larvae Infected by Hypervirulent Strains of *K. pneumoniae*.

Statistical test	Chi-square	Degrees of freedom (df)	P-Value	Significance
Log-rank (Mantel-Cox)	208.8	9	< 0.0001	**** (highly significant)
Gehan-Breslow-Wilcoxon	189.6	9	< 0.0001	**** (highly significant)
Logrank for trend	10.70	1	0.0011	** (significant)

5. DISCUSSION

The genetic diversity and virulence of *K. pneumoniae* have been subjects of interest in several previous studies. In line with prior research (Lee et al., 2017), a wide variety of virulence genes have been found in the strains of *K. pneumoniae* under study. One such gene is *kfuBC*, responsible for ferric iron uptake, which has been shown to be more prevalent in hvKp strains compared to cKp (Russo et al., 2009). This is consistent with our findings, as this gene is among the most prevalent (51.16%) in our hypervirulent *K. pneumoniae* strains. However, it should be noted that the mere detection of virulence genes does not ensure their functional activity, as their expression may be regulated by various genetic and environmental factors, and their presence in the genome does not guarantee their transcription and translation into functional proteins.

Additionally, other prevalent genes such as *wabG*, *ureA*, *fim*, and *uge* were identified among our results. For example, *wabG* participates in bacterial capsule biosynthesis, a crucial structure for resistance to phagocytosis and evasion of the host immune system. Conversely, *ureA* encodes a urease subunit, an enzyme relevant in bacterial adaptation to acidic environments and colonization of the urinary tract. The *fim* and *uge* genes are involved in adhesion to host cells and biofilm formation, phenomena facilitating infection and bacterial persistence.

Capsule genes are chromosomal and largely conserved across species, but there is variation in capsule polysaccharide components, which forms the basis for their typing. The different polysaccharide variants resulting from genetic differences are termed K antigens and have been serologically categorized. Currently, capsule synthesis *wzi* genes sequencing is the predominant methodology, and at least 134 distinct K loci have been identified. The most common capsule locus associated with hvKp is K1, followed by K2, K5, and K57. When comparing the *K. pneumoniae* capsular types results obtained in our study with those reported in other articles, both similarities and significant differences are observed. In our study, the most prevalent capsule genes were *magA* (K1) and *wzy_K2*, at 25% and 32.5%, respectively. This agrees with previously cited studies. However, unlike the literature where *wzx_K5* is highly prevalent in hvKp strains, no strains with this capsular type were found in our study.

Despite the high frequency of K1 and K2 loci in hvKp isolates, capsule type alone does not fully explain hypervirulence. These capsule types coexist with other virulence genes, many of which have been mentioned, and attempts to genetically exchange capsule loci between isolates have yielded mixed results. Swapping the capsule from a less virulent strain with that from an hvKp strain does not completely establish the virulent phenotype in mouse models, suggesting that the capsule is not the sole driver of virulence. However, it plays an important role in preventing

phagocytosis and in enhancing the survival and dissemination of hvKp. K1 hvKp isolates have been shown to be more resistant than cKp isolates to extracellular and intracellular neutrophil-mediated death. It is likely that the evolution of hvKp with certain capsule types is the result of the advantages conferred by these different capsule structures.

The analysis of resistance genes in our hvKp strains revealed that the most prevalent genes were *oqxA/B* and *oqxB*, encoding the OqxAB efflux pump system responsible for releasing a wide variety of antibiotics from the bacteria, including quinolones, aminoglycosides, and tetracyclines. The presence of this resistance gene in hypervirulent *K. pneumoniae* strains significantly contributes to their ability to evade the effects of antibiotics and survive in hostile environments, such as the human body during an infection.

Furthermore, there was also a high prevalence of *fosA* and bla_{SHV}, in their different allelic variants. The former is associated with resistance to antibiotics of the fosfomycin family, while the latter encodes an extended-spectrum beta-lactamase (ESBL) capable of hydrolyzing cephalosporins and penicillins. The prevalence of bla_{SHV} (85.3%) is consistent with the literature. It is considered intrinsic to *K. pneumoniae*, forming part of its core genome, and also confers resistance to first-generation penicillins and cephalosporins. There are few exceptions of *K. pneumoniae* isolates that do not contain it, including some with K2-ST66, which were precisely found in three isolates in this study (1012420, 1033468, and 50368567), which were indeed negative in the resistance gene heatmap (Figure 5). This finding coincides with previous studies, such as that of Yao et al., 2020, which also found a high prevalence of bla_{SHV} in their *K. pneumoniae* isolates, indicating that this gene is a key determinant in beta-lactam antibiotic resistance.

$bla_{\text{OXA-48}}$ and $bla_{\text{CTX-M-15}}$ are resistance genes with low prevalence in our work, but they are important due to their ability to confer resistance to key antibiotics, further complicating the treatment of bacterial infections, including those caused by hypervirulent *K. pneumoniae*. The presence of $bla_{\text{OXA-48}}$ confers resistance to carbapenems, significantly limiting treatment options and increasing severity and mortality. On the other hand, the $bla_{\text{CTX-M-15}}$ gene encodes an ESBL that hydrolyses third-generation cephalosporins, such as ceftriaxone and ceftazidime.

Another study by Gu et al., 2018 highlighted the coexistence of resistance genes and virulence genes in hvKp strains, similar to this work, suggesting that the combination of high virulence and antimicrobial resistance significantly complicates the treatment of infections caused by these strains.

The results obtained in this study regarding MLST (Multi-Locus Sequence Typing) are consistent with existing literature describing a typing screening for *K. pneumoniae*. For example, the

prevalence of ST23 is consistent with previous studies identifying this type as common in hypervirulent strains of *K. pneumoniae*. ST23, like others present in this work such as ST86, is associated with hvKp strains. If we observe isolate ST86 (1157007) in Figure 4, it presents many of the genes associated with virulence such as *rmpA*, *wzy_K2*, *fim*, *aerobactin*, and *peg-344* (Russo et al., 2019; Shon et al., 2013). Furthermore, ST23 has been shown to be strongly associated with capsular type K1, and if we observe Figure 4, we can see that ST23 strains such as 943123, 789428, and 752102 are positive for *magA*.

Our findings regarding biofilm production in *K. pneumoniae* strains are consistent with several previous studies that have investigated this phenomenon in various clinical and environmental contexts. For example, Vuotto et al., 2017 observed a similar distribution of *K. pneumoniae* strains in different categories of biofilm production, with comparable percentages of non-producers, weak producers, moderate producers, and strong producers, suggesting that variability in biofilm production is a common feature in different populations of *K. pneumoniae* and is not limited to a single set of clinical isolates.

Although it was expected that all strains in our study, being hypermucoid and hypervirulent, would exhibit high biofilm production, the results show that this is not always the case. Biofilm production and hypervirulence may be influenced by different genetic and regulatory mechanisms. For example, Choi et al., 2020 demonstrated that specific genetic factors, such as the presence of certain plasmids, can significantly modulate biofilm formation capacity in *K. pneumoniae*. This finding emphasizes the complexity of the genetic regulation of these phenotypes and suggests that more studies are needed to better understand the specific factors that influence biofilm production and virulence.

Our results also reflect the findings of Paczosa et al., 2016, who indicated that *K. pneumoniae* strains capable of forming biofilm had a greater capacity to colonize the respiratory tract and cause invasive infections in animal models. In our study, strains with high biofilm production, such as isolates 56523365 and 754209 ($bla_{\text{OXA-48}}$), showed a high mortality rate in *G. mellonella* infection, while strains with low biofilm production, such as Basurto 9, had a low mortality rate. These findings highlight the importance of biofilm production in the pathogenicity of *K. pneumoniae* and its ability to cause severe infections.

Also, biofilm production in *K. pneumoniae* can be affected by external factors, such as the presence of antibiotics and the composition of the culture medium. For example, the study by Wang et al., 2020 showed that biofilm formation can be induced by environmental stress conditions, which could have significant implications for the treatment of infections caused by this bacterium.

As described in this work, flagellum-dependent bacterial motility is necessary for the initial stages of biofilm formation. Once bacteria have adhered to a surface and formed a biofilm, motility may be reduced or even stopped due to physical immobilization within the extracellular matrix. Therefore, we could assume that higher biofilm production leads to lower motility in those bacteria. However, some bacteria may retain the ability to move within the three-dimensional structure of the biofilm, allowing redistribution and colonization of new areas within it.

Furthermore, bacterial motility can influence the structure of the biofilm. Highly mobile bacteria can quickly colonize new surfaces and form denser and more heterogeneous biofilms. Thus, the relationship between biofilm and bacterial motility is complex and may vary depending on bacterial species, environmental conditions, or surface characteristics to which they adhere.

According to the results obtained in the previous sections on biofilm and motility of *K. pneumoniae*, we compared both to see if there was a relationship. We calculated the Pearson coefficient (R) and obtained very low values, indicating that the correlation between these variables is weak (Figure 12).

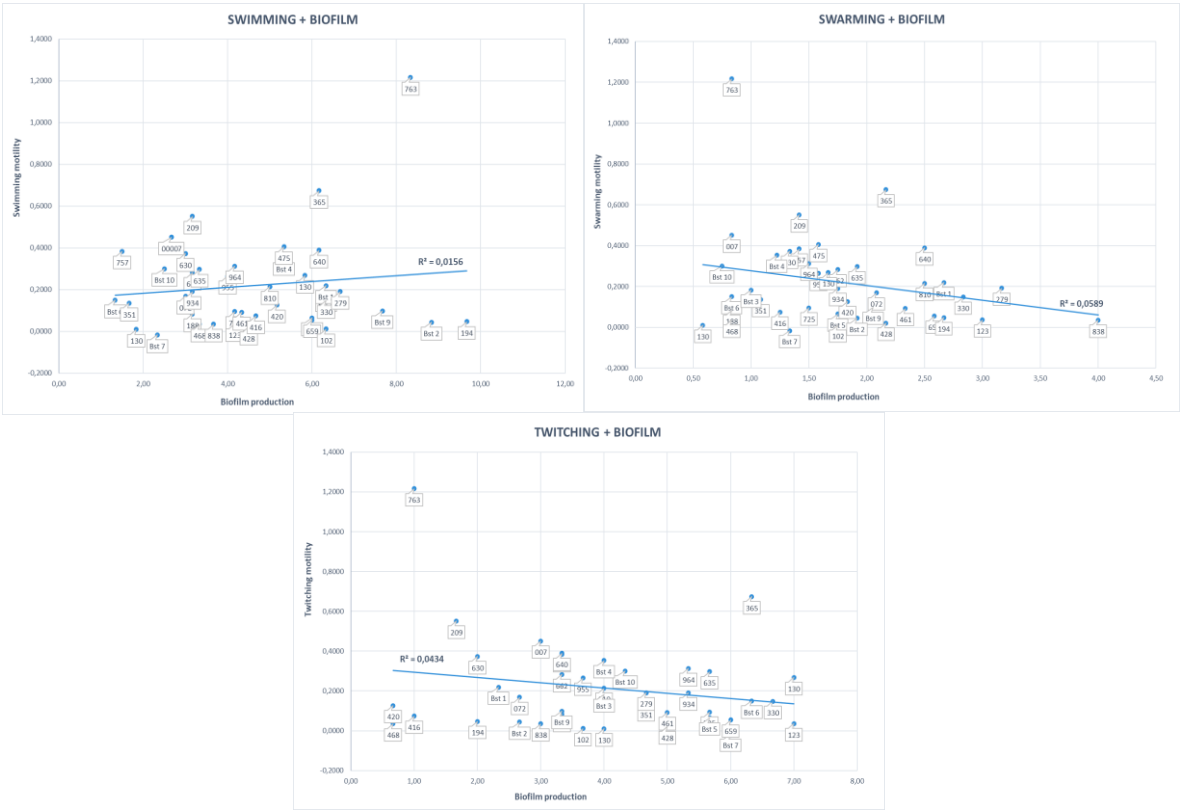

Figure 12. Correlation between motility and biofilm Formation in *K. pneumoniae* strains using Pearson's Correlation Coefficient (R).

As mentioned in the results section, only 4.65% of the 43 isolates of *K. pneumoniae* were considered non-motile in swimming motility, suggesting a significant capacity for movement in

aqueous media, surpassing previous expectations based on earlier studies that generally described this bacterium as generally non-motile (Carabarin-Lima et al., 2016). However, there is also a study in which swimming motility was examined in *Klebsiella oxytoca*, where this bacterium appears to exhibit this type of motility. The swimming of *K. oxytoca* isolates was evaluated in TSB (pH 8.5, 0.5% NaCl, 0.25% agar) at 37°C for 72 hours, unlike ours, which were left in the incubator at 37°C for 20 hours (Sun et al., 2024).

In contrast, a higher proportion of non-motile strains were observed in swarming motility compared to swimming and twitching. These findings provide a new perspective on the heterogeneity of motility in *K. pneumoniae*, highlighting the importance of swimming, which could be crucial for colonization of aqueous surfaces and dissemination in clinical settings.

However, it is important to note that the results of twitching motility are particularly controversial due to the variability in different measurement techniques and experimental conditions in various studies. Although the understanding of this phenomenon in *K. pneumoniae* is limited, similar research in bacteria such as *P. aeruginosa* (Haley et al., 2014) and *Acinetobacter baumannii* (Vijayakumar et al., 2016) has shown that twitching motility, mediated by type IV pili, plays an important role in biofilm formation and colonization of abiotic surfaces. Moreover, in species such as *Neisseria meningitidis*, twitching motility and surface colonization have also been studied (Carbonnelle et al., 2006; Guerry et al., 2007).

The frequency of conjugation between bacteria, such as *K. pneumoniae* and *E. coli*, is influenced by a series of both biotic and abiotic factors. These factors include bacterial growth phase, cell density, donor-recipient ratio, nutrient concentrations, temperature, pH, and mating duration. In addition, the choice of donor and recipient bacterial species, the type of plasmid involved, and the experimental method used also have a significant impact on the observed conjugation frequency (Singh et al., 2023).

Our findings present a notable discrepancy with similar conjugation studies conducted under comparable conditions. The same recipient strain, the same antibiotic selection for transconjugants, and the same CFU/ml were used; however, a different donor strain (although also belonging to *K. pneumoniae*), a different plasmid (although both with OXA-48), and a different medium (LB broth) were used (Gottig et al., 2015). The reported in vitro conjugation frequency of OXA-48 in *K. pneumoniae* to *E. coli* J53 AZ^R in the mentioned study was 8.7×10^{-7}, in contrast to the conjugation frequency in this study, which was 8.65×10^{-2}. When comparing both frequencies, it is evident that the conjugation frequency in our study is significantly higher. However, it is important to note that this discrepancy could be due to small experimental variations, which can have a substantial impact on conjugation efficiency.

Conjugation studies were also conducted in vivo in *G. mellonella* and mice in this article, where conjugation frequencies increased; nevertheless, our frequency remained higher. The successful transfer of the pOXA-48-Kp754209 plasmid to *E. coli* J53 underlines the ease with which resistance genes can spread between different bacterial species. This phenomenon is concerning from a clinical perspective, as it can lead to the emergence of multidrug-resistant strains that limit available therapeutic options.

Infection assays with *G. mellonella* provided valuable insights into the relative virulence of different *K. pneumoniae* strains, including some carrying important resistance genes such as $bla_{\text{OXA-48}}$ and $bla_{\text{CTX-M-15}}$. The results showed significant variations in larval survival depending on the infecting strain, highlighting the crucial influence of bacterial virulence on pathogenicity.

In a study by Insua et al., 2013, the virulence of *K. pneumoniae* strains in *G. mellonella* was evaluated, observing significant differences in larval survival depending on the resistance profile of the strains. Strains carrying the bla_{KPC} gene showed higher virulence compared to those that did not. These results are consistent with the findings of our study, where significant variability in larval survival was also observed depending on the infecting strain and genetic resistance profiles. A notable difference is that in Insua et al.'s study, 75% of the larvae died at 24 hours and 100% at 72 hours post-infection, whereas in the present study, around 50% of the larvae survived at 72 hours post-infection even with the most virulent strains (excluding the positive control PAO1). This discrepancy could be due to the quantity of CFU injected, being 10^6 in their study and 10^5 in ours, which could explain the higher virulence observed in their case.

The *G. mellonella* model has also proven useful for evaluating the pathogenic potential of *K. pneumoniae*, showing a strong correlation with virulence previously determined in the mouse pneumonia infection model. Additionally, there is evidence that *K. pneumoniae* infection in *G. mellonella* models some of the known characteristics of pneumonia caused by this bacterium, including cell necrosis resulting from an intense inflammatory response triggered by high bacterial loads (Podschun et al., 1998).

Another relevant study is that of Wand et al., 2013, which investigated the virulence of different *K. pneumoniae* strains in *G. mellonella*. They found that the expression of certain virulence factors, such as capsule and fimbriae, significantly influenced larval survival. Strains with higher capsule expression showed significantly higher virulence. However, in our study, the strains with the highest mortality rates were 56523365 and 754209, which did not present any studied virulence capsulotype, although both were positive for the *fim* gene (fimbriae). On the other hand, strain 943123, which showed lower mortality, presented capsulotype K1 (*magA*) and was also positive for *fim*.

6. LIMITATIONS

This study has several notable limitations that should be taken into account when interpreting the results. Firstly, only the presence and absence of genes were measured without assessing their expression. Detecting a virulence gene does not necessarily imply its active role in pathogenesis, as its expression can be influenced by various environmental and genetic factors. Furthermore, its presence in the genome does not ensure transcription and translation into functional proteins.

Moreover, biofilm production was assessed using a colorimetric method, which, although widely used, may not fully capture the complexity and three-dimensional architecture of biofilms under natural conditions. Environmental factors affecting biofilm production, such as nutrient availability and stress conditions, were not evaluated.

In the case of bacterial motility studies, multiple factors including the presence of pili, expression of motility proteins, and environmental interactions influence the results. Standardizing motility measurements can be challenging and may be affected by variability in experimental conditions, including the components of the medium used. Even minor discrepancies in these components could lead to significant differences in outcomes.

Another consideration is the limitation to using only one *E. coli* recipient strain in the conjugation assay, which restricts the generalizability of the results to other bacterial species. Controlled laboratory conditions may not fully replicate the complexities of a real clinical environment, where various factors can influence plasmid transfer dynamics.

Lastly, the use of *G. mellonella* as an animal model may not fully reflect human pathogenicity due to anatomical, physiological, and immunological differences. Besides, the small number of strains studied may limit the generalizability of the findings.

7. CONCLUSIONS

The results of this study underscore the significant threat posed by hypervirulent *Klebsiella pneumoniae* (hvKp) due to its multiple virulence and resistance mechanisms. The high prevalence of key virulence genes such as *magA*, *K2wzy*, and *fim*, alongside resistance genes $bla_{\text{OXA-48}}$ and bla_{SHV}, highlights the complex genetic landscape that contributes to the pathogenicity and resistance of hvKp. The observed variability in biofilm production, despite standardized conditions, indicates that numerous factors influence its formation, complicating the development of effective treatment strategies. Moreover, the unexpected motility of strains typically considered non-motile emphasizes the adaptive capabilities of hvKp, enhancing its ability to colonize and infect hosts.

The successful conjugation of an OXA-48 encoding plasmid into a multidrug-resistant hvKp isolate exacerbates the challenge of antimicrobial resistance. Infection assays using *G. mellonella* larvae confirmed the high virulence of the selected strains, suggesting that hvKp can cause severe infections even in previously healthy individuals.

We can conclude that our strains are highly likely to be hypervirulent based on all the results obtained and the consulted literature. However, due to the previously discussed limitations, we cannot assert this definitively, and further research is needed to confirm it.

Future research should focus on the environmental factors affecting biofilm formation and the underlying mechanisms of hvKp motility. In addition, expanding conjugation studies to include a broader range of bacterial species and clinical conditions will provide a more comprehensive understanding of plasmid transfer dynamics. It would also be beneficial to conduct expression studies of virulence and resistance genes, as well as microscopy studies to determine if these strains possess flagella or only flagellar genes. There is limited information on motility studies in *K. pneumoniae*, and further investigation into this area is crucial as it influences virulence.

The future of multidrug-resistant bacteria is concerning and requires extensive research to develop effective control and treatment strategies. The development of new therapeutic approaches targeting the unique virulence and resistance mechanisms of hvKp is imperative to mitigate the public health threat posed by this pathogen. However, it is essential first to understand and control all the virulence and resistance factors discussed in this work.

8. ACKNOWLEDGMENTS

I would like to express my sincere gratitude to all the individuals who contributed to the realization of this project named KLEVIRE and, more specifically, to my Master's thesis. Firstly, I am deeply thankful to my supervisor, Alain Antonio Ocampo Sosa, for entrusting me with this study and for his guidance throughout the work. Likewise, I extend my gratitude to my co-supervisor, Sergio García Fernández, for his guidance and availability.

Additionally, I want to express my appreciation to the entire Servicio de Microbiología del Hospital Universitario Marqués de Valdecilla-IDIVAL and especially to Domingo Fernández Vecilla, Pedro Bustamante de la Escalera, Jorge Rodríguez Grande, Ana Navarro Alcalde, and especially to Nuria Fraile Valcárcel, for her dedication, teaching, and support throughout all the practices. Her experience and commitment were fundamental for the development of this project.

Finally, I wish to express my deep gratitude to my family and friends for their constant support and infinite patience. I feel very fortunate to have them by my side. Their unwavering support and the confidence they have given me have been crucial on this journey.

9. REFERENCES

1) Alav, I., Pordelkhaki, P., De Resende, P. E., Partington, H., Gibbons, S., Lord, R. M., & Buckner, M. M. C. (2024). Cobalt complexes modulate plasmid conjugation in *Escherichia coli* and *Klebsiella pneumoniae*. *Scientific Reports, 14*(1). https://doi.org/10.1038/s41598-024-58895-x

2) Balestrino, D., Ghigo, J., Charbonnel, N., Haagensen, J. A. J., & Forestier, C. (2008). The characterization of functions involved in the establishment and maturation of *Klebsiella pneumoniae* in vitro biofilm reveals dual roles for surface exopolysaccharides. *Environmental Microbiology, 10*(3), 685-701. https://doi.org/10.1111/j.1462-2920.2007.01491.x

3) Balestrino, D., Haagensen, J. A. J., Rich, C., & Forestier, C. (2005). Characterization of Type 2 Quorum Sensing in *Klebsiella pneumoniae* and Relationship with Biofilm Formation. *Journal Of Bacteriology, 187*(8), 2870-2880. https://doi.org/10.1128/jb.187.8.2870-2880.2005

4) Bialek-Davenet, S., Criscuolo, A., Ailloud, F., Passet, V., Jones, L., Delannoy-Vieillard, A., Garin, B., Hello, S. L., Arlet, G., Nicolas-Chanoine, M., Decré, D., & Brisse, S. (2014). Genomic Definition of Hypervirulent and Multidrug-Resistant *Klebsiella pneumoniae* Clonal Groups. *Emerging Infectious Diseases, 20*(11), 1812-1820. https://doi.org/10.3201/eid2011.140206

5) Carabarin-Lima, A., León-Izurieta, L., Del Carmen Rocha-Gracia, R., Castañeda-Lucio, M., Torres, C., Gutiérrez-Cazarez, Z., González-Posos, S., De la Peña, C. F. M., Martinez-Laguna, Y., & Lozano-Zarain, P. (2016). First evidence of polar flagella in *Klebsiella pneumoniae* isolated from a patient with neonatal sepsis. *Journal Of Medical Microbiology/Journal Of Medical Microbiology, 65*(8), 729-737. https://doi.org/10.1099/jmm.0.000291

6) Carbonnelle, E., Helaine, S., Nassif, X., & Pelicic, V. (2006). A systematic genetic analysis in *Neisseria meningitidis* defines the Pil proteins required for assembly, functionality, stabilization and export of type IV pili. *Molecular Microbiology, 61*(6), 1510-1522. https://doi.org/10.1111/j.1365-2958.2006.05341.x

7) Chen, J., Zhang, H., & Liao, X. (2023). Hypervirulent *Klebsiella pneumoniae*. *Infection And Drug Resistance, Volume 16*, 5243-5249. https://doi.org/10.2147/idr.s418523

8) Choby, J. E., Howard-Anderson, J., & Weiss, D. S. (2019). Hypervirulent *Klebsiella pneumoniae* – clinical and molecular perspectives. *Journal Of Internal Medicine*, 287(3), 283-300. https://doi.org/10.1111/joim.13007

9) Choi, M., Hegerle, N., Nkeze, J., Sen, S., Jamindar, S., Nasrin, S., Sen, S., Permala-Booth, J., Sinclair, J., Tapia, M. D., Johnson, J. K., Mamadou, S., Thaden, J. T., Fowler, V. G., Aguilar, A., Terán, E., Decre, D., Morel, F., Krogfelt, K. A.,Tennant, S. M. (2020). The Diversity of Lipopolysaccharide (O) and Capsular Polysaccharide (K) Antigens of Invasive *Klebsiella pneumoniae* in a Multi-Country Collection. *Frontiers In Microbiology*, *11*. https://doi.org/10.3389/fmicb.2020.01249

10) Carabin-Lima, A., León-Izurieta, L., Del Carmen Rocha-García, R., Castañeda-Lucio, M., Torres, C., Gutiérrez-Cásarez, Z.,González-Posos, S., De la Peña, C. F. M., Martínez-Laguna, Y., & Lozano-Zaraín, P. (2016). First evidence of polar flagella in *Klebsiella pneumoniae* isolated from a patient with neonatal sepsis. *Journal Of Medical Microbiology*, 65(8), 729-737. https://doi.org/10.1099/jmm.0.000291

11) Clegg, S., & Murphy, C. N. (2016). Epidemiology and Virulence of *Klebsiella pneumoniae*. *Microbiology Spectrum*, *4*(1). https://doi.org/10.1128/microbiolspec.uti-0005-2012

12) Díaz-Ríos, C., Hernández, M., Abad, D., Álvarez-Montes, L., Varsaki, A., Iturbe Fernández, D., Calvo, J., & Ocampo-Sosa, A. A. (2021). New Sequence Type ST3449 in Multidrug-Resistant *Pseudomonas aeruginosa* Isolates from a Cystic Fibrosis Patient. *Antibiotics*, *10*(5), 491. https://doi.org/10.3390/antibiotics10050491

13) Fang, C., Chuang, Y., Shun, C., Chang, S., & Wang, J. (2004). A Novel Virulence Gene in *Klebsiella pneumoniae* Strains Causing Primary Liver Abscess and Septic Metastatic Complications. *The Journal Of Experimental Medicine*, *199*(5), 697-705. https://doi.org/10.1084/jem.20030857

14) Gomes, A. É. I., Pacheco, T., Da Silva Dos Santos, C., Pereira, J. A., Ribeiro, M. L., Darrieux, M., & Ferraz, L. F. C. (2021). Functional Insights From KpfR, a New Transcriptional Regulator of Fimbrial Expression That Is Crucial for *Klebsiella pneumoniae* Pathogenicity. *Frontiers In Microbiology*, 11. https://doi.org/10.3389/fmicb.2020.601921

15) Gottig, S., Gruber, T. M., Stecher, B., Wichelhaus, T. A., & Kempf, V. A. J. (2015). In Vivo Horizontal Gene Transfer of the Carbapenemase OXA-48 During a Nosocomial Outbreak. Clinical Infectious *Diseases/Clinical Infectious Diseases (Online. University Of Chicago. Press)*, *60*(12), 1808-1815. https://doi.org/10.1093/cid/civ191

16) Gu, D., Dong, N., Zheng, Z., Lin, D., Huang, M., Wang, L., Chan, E. W., Shu, L., Yu, J., Zhang, R., & Chen, S. (2018). A fatal outbreak of ST11 carbapenem-resistant hypervirulent *Klebsiella pneumoniae* in a Chinese hospital: a molecular epidemiological study. *Lancet. Infectious Diseases*, *18*(1), 37-46. https://doi.org/10.1016/s1473-3099(17)30489-9

17) Guerra, M. E. S., Destro, G., Vieira, B., Lima, A. S., Ferraz, L. F. C., Håkansson, A. P., Darrieux, M., & Converso, T. R. (2022). *Klebsiella pneumoniae* Biofilms and Their Role in Disease Pathogenesis. *Frontiers In Cellular And Infection Microbiology*, *12*. https://doi.org/10.3389/fcimb.2022.877995

18) Guerry, P. (2007). Campylobacter flagella: not just for motility. *Trends In Microbiology*, 15(10), 456-461. https://doi.org/10.1016/j.tim.2007.09.006

19) Guilhen, C., Miquel, S., Charbonnel, N., Joseph, L., Carrier, G., Forestier, C., & Balestrino, D. (2019). Colonization and immune modulation properties of *Klebsiella pneumoniae* biofilm-dispersed cells. *Npj Biofilms And Microbiomes*, 5(1). https://doi.org/10.1038/s41522-019-0098-1

20) Haley, C. L., Kruczek, C., Qaisar, U., Colmer-Hamood, J. A., & Hamood, A. N. (2014). Mucin inhibits *Pseudomonas aeruginosa* biofilm formation by significantly enhancing twitching motility. *Canadian Journal Of Microbiology*, *60*(3), 155-166. https://doi.org/10.1139/cjm-2013-0570

21) Hall-Stoodley, L., Costerton, J. W., & Stoodley, P. (2004). Bacterial biofilms: from the Natural environment to infectious diseases. *Nature Reviews. Microbiology*, *2*(2), 95-108. https://doi.org/10.1038/nrmicro821

22) Hamprecht, A., Sommer, J., Willmann, M., Brender, C., Stelzer, Y., Krause, F. F., Tsvetkov, T., Wild, F., Riedel-Christ, S., Kutschenreuter, J., Imirzalioglu, C., Gonzaga, A., Nübel, U., & Göttig, S. (2019). Pathogenicity of Clinical OXA-48 Isolates and Impact of the OXA-48 IncL Plasmid on Virulence and Bacterial Fitness. *Frontiers In Microbiology*, *10*. https://doi.org/10.3389/fmicb.2019.02509

23) Han, Y., Wen, X., Zhao, W., Cao, X., Wen, J., Wang, J., Hu, Z., & Zheng, W. (2022). Epidemiological characteristics and molecular evolution mechanisms of carbapenem-resistant hypervirulent *Klebsiella pneumoniae*. *Frontiers In Microbiology*, *13*. https://doi.org/10.3389/fmicb.2022.1003783

24) Insua, J. L., Llobet, E., Moranta, D., Pérez-Gutiérrez, C., Axelsson, T., Garmendia, J., & Bengoechea, J. A. (2013). Modeling Klebsiella pneumoniae Pathogenesis by Infection of the Wax Moth *Galleria mellonella*. *Infection And Immunity*, *81*(10), 3552-3565. https://doi.org/10.1128/iai.00391-13

25) Jian-Li, W., Yuan-Yuan, S., Shou-Yu, G., Fei-Fei, D., Jia-Yu, Y., Xue-Hua, W., Yong-Feng, Z., Shi-Jin, J., & Zhi-Jing, X. (2017). Serotype and virulence genes of *Klebsiella pneumoniae* isolated from mink and its pathogenesis in mice and mink. Scientific Reports, 7(1). https://doi.org/10.1038/s41598-017-17681-8

26) Kinosita, Y., & Sowa, Y. (2023). Flagellar polymorphism-dependent bacterial swimming motility in a structured environment. *Biophysics And Physicobiology*, *20*(2), n/a. https://doi.org/10.2142/biophysico.bppb-v20.0024

27) Kocsis, B. (2023). Hypervirulent *Klebsiella pneumoniae*: An update on epidemiology, detection and antibiotic resistance. *Acta Microbiologica Et Immunologica Hungarica, 70*(4), 278-287. https://doi.org/10.1556/030.2023.02186

28) Lee, C., Lee, J. H., Park, K. S., Kim, Y. B., Jeong, B. C., & Lee, S. H. (2016). Global Dissemination of Carbapenemase-Producing *Klebsiella pneumoniae*: Epidemiology, Genetic Context, Treatment Options, and Detection Methods. *Frontiers In Microbiology*, *7*. https://doi.org/10.3389/fmicb.2016.00895

29) Lee, I. R., Molton, J. S., Wyres, K. L., Gorrie, C., Wong, J., Hoh, C. H., Teo, J., Kalimuddin, S., Lye, D. C., Archuleta, S., Holt, K. E., & Gan, Y. (2016). Differential host susceptibility and bacterial virulence factors driving *Klebsiella* liver abscess in an ethnically diverse population. *Scientific Reports, 6*(1). https://doi.org/10.1038/srep29316

30) Mendes, G., Santos, M. L., Ramalho, J. F., Duarte, A., & Caneiras, C. (2023). Virulence factors in carbapenem-resistant hypervirulent *Klebsiella pneumoniae*. *Frontiers In Microbiology, 14*. https://doi.org/10.3389/fmicb.2023.1325077

31) O'Toole, G. A., & Kolter, R. (1998). Initiation of biofilm formation in *Pseudomonas* fluorescens WCS365 proceeds via multiple, convergent signalling pathways: a genetic analysis. *Molecular Microbiology*, *28*(3), 449-461. https://doi.org/10.1046/j.1365-2958.1998.00797.x

32) Paczosa, M. K., & Mecsas, J. (2016). Klebsiella pneumoniae: Going on the Offense with a Strong Defense. *Microbiology And Molecular Biology Reviews*, *80*(3), 629-661. https://doi.org/10.1128/mmbr.00078-15

33) Piperaki, E., Syrogiannopoulos, G. A., Tzouvelekis, L. S., & Daikos, G. L. (2017). *Klebsiella pneumoniae*: Virulence, Biofilm and Antimicrobial Resistance. *The Pediatric Infectious Disease Journal/ The Pediatric Infectious Disease Journal*, *36*(10), 1002-1005. https://doi.org/10.1097/inf.0000000000001675

34) Podschun, R., & Ullmann, U. (1998). *Klebsiell*a spp. as Nosocomial Pathogens: Epidemiology, Taxonomy, Typing Methods, and Pathogenicity Factors. *Clinical Microbiology Reviews*, *11*(4), 589-603. https://doi.org/10.1128/cmr.11.4.589

35) Russo, T. A., & Marr, C. M. (2019). Hypervirulent *Klebsiella pneumoniae*. *Clinical Microbiology Reviews*, *32*(3). https://doi.org/10.1128/cmr.00001-19

36) Saxena, P., Joshi, Y., Rawat, K., & Bisht, R. (2018). Biofilms: Architecture, Resistance, Quorum Sensing and Control Mechanisms. *Indian Journal Of Microbiology/Indian Journal Of Microbiology (Print)*, *59*(1), 3-12. https://doi.org/10.1007/s12088-018-0757-6

37) Shon, A. S., Bajwa, R. P., & Russo, T. A. (2013). Hypervirulent (hypermucoviscous) *Klebsiella pneumoniae*. *Virulence*, *4*(2), 107-118. https://doi.org/10.4161/viru.22718

38) Singh, S., Pathak, A., Fatima, N., Sahu, C., & Prasad, K. N. (2023). Characterisation of OXA-48-like carbapenemases in Escherichia coli and *Klebsiella pneumoniae* from North India. 3 *Biotech*, *13*(5). https://doi.org/10.1007/s13205-023-03537-8

39) Sun, S., Gu, T., Ou, Y., Wang, Y., Xie, L., & Chen, L. (2024). Environmental Compatibility and Genome Flexibility of *Klebsiella oxytoca* Isolated from Eight Species of Aquatic Animals. *Diversity*, *16*(1), 30. https://doi.org/10.3390/d16010030

40) Vijayakumar, S., Rajenderan, S., Laishram, S., Anandan, S., Balaji, V., & Biswas, I. (2016). Biofilm Formation and Motility Depend on the Nature of the *Acinetobacter baumannii* Clinical Isolates. *Frontiers In Public Health*, *4*. https://doi.org/10.3389/fpubh.2016.00105

41) Vuotto, C., Longo, F., Pascolini, C., Donelli, G., Balice, M. P., Libori, M. F., Tiracchia, V., Salvia, A., & Varaldo, P. E. (2017). Biofilm formation and antibiotic resistance in *Klebsiella pneumoniae* urinary strains. *Journal Of Applied Microbiology*, *123*(4), 1003-1018. https://doi.org/10.1111/jam.13533

42) Wahl, A., Fischer, M. A., Klaper, K., Müller, A., Borgmann, S., Friesen, J., Hunfeld, K., Ilmberger, A., Kolbe-Busch, S., Kresken, M., Lippmann, N., Lübbert, C., Marschner, M., Neumann, B., Pfennigwerth, N., Probst-Kepper, M., Rödel, J., Chulze, M. H., Zautner, A. E., Pfeifer, Y. (2024). Presence of hypervirulence-associated determinants in *Klebsiella pneumoniae* from hospitalised patients in Germany. *International Journal Of Medical Microbiology*, 151601. https://doi.org/10.1016/j.ijmm.2024.151601

43) Wand, M. E., Müller, C. M., Titball, R. W., & Michell, S. L. (2011). Macrophage and *Galleria mellonella* infection models reflect the virulence of naturally occurring isolates of *B. pseudomallei*, *B. thailandensis* and *B. oklahomensis*. *BMC Microbiology*, *11*(1). https://doi.org/10.1186/1471-2180-11-11

44) Wang, G., Zhao, G., Chao, X., Xie, L., & Wang, H. (2020). The Characteristic of Virulence, Biofilm and Antibiotic Resistance of *Klebsiella pneumoniae*. *International Journal Of Environmental Research And Public Health/International Journal Of Environmental Research And Public Health*, *17*(17), 6278. https://doi.org/10.3390/ijerph17176278

45) Wyres, K. L., Lam, M. M. C., & Holt, K. E. (2020). Population genomics of *Klebsiella pneumoniae*. *Nature Reviews. Microbiology*, 18(6), 344-359. https://doi.org/10.1038/s41579-019-0315-1

46) Yao, H., Qin, S., Chen, S., Shen, J., & Du, X. (2018). Emergence of carbapenem-resistant hypervirulent *Klebsiella pneumoniae*. *Lancet. Infectious Diseases/˜The œLancet. Infectious Diseases*, 18(1), 25. https://doi.org/10.1016/s1473-3099(17)30628-x

47) Zegadło, K., Gieroń, M., Żarnowiec, P., Durlik-Popińska, K., Kręcisz, B., Kaca, W., & Czerwonka, G. (2023). Bacterial Motility and Its Role in Skin and Wound Infections. *International Journal Of Molecular Sciences*, *24*(2), 1707. https://doi.org/10.3390/ijms24021707

48) Zhu, J., Wang, T., Chen, L., & Du, H. (2021). Virulence Factors in Hypervirulent *Klebsiella pneumoniae*. *Frontiers In Microbiology*, *12*. https://doi.org/10.3389/fmicb.2021.642484